AEDC-TR-77-72

cy. 2

JUL 1 1 1977

COMPUTER PROGRAM FOR CALCULATION OF SEPARATED TURBULENT FLOWS ON AXISYMMETRIC AFTERBODIES

NIELSEN ENGINEERING & RESEARCH, INC.
510 CLYDE AVENUE
MOUNTAIN VIEW, CALIFORNIA 94043

June 1977

Final Report for Period 15 March 1976 to 15 April 1977

Prepared for

DIRECTORATE OF TECHNOLOGY
ARNOLD ENGINEERING DEVELOPMENT CENTER
AIR FORCE SYSTEMS COMMAND
ARNOLD AIR FORCE STATION, TENNESSEE 37389

NOTICES

This final report was submitted by Nielsen Engineering & Research, Inc., 510 Clyde Ave., Mountain View, California 94043, under contract F40600-76-C-0009, with the Arnold Engineering Development Center, Arnold Air Force Station, Tennessee 37389. Mr. Elton Thompson was the AEDC Project Engineer.

APPROVAL STATEMENT

This technical report has been reviewed and is approved for publication.

FOR THE COMMANDER

Elton R. Thompson

ELTON R. THOMPSON
Research and Development
Division
Directorate of Technology

Robert O Dietz

ROBERT O. DIETZ
Director of Technology

REPORT DOCUMENTATION PAGE		READ INSTRUCTIONS BEFORE COMPLETING FORM
1. REPORT NUMBER AEDC-TR-77-72	2. GOVT ACCESSION NO.	3. RECIPIENT'S CATALOG NUMBER
4. TITLE (and Subtitle) COMPUTER PROGRAM FOR CALCULATION OF SEPARATED TURBULENT FLOWS ON AXISYMMETRIC AFTERBODIES		5. TYPE OF REPORT & PERIOD COVERED Final Report - March 15, 1976 to April 15, 1977 6. PERFORMING ORG. REPORT NUMBER NEAR TR 131
7. AUTHOR(s) Gary D. Kuhn		8. CONTRACT OR GRANT NUMBER(s) F40600-76-C-0009
9. PERFORMING ORGANIZATION NAME AND ADDRESS Nielsen Engineering & Research, Inc. 510 Clyde Avenue Mountain View, California 94043		10. PROGRAM ELEMENT, PROJECT, TASK AREA & WORK UNIT NUMBERS Program Element 65807F
11. CONTROLLING OFFICE NAME AND ADDRESS Arnold Engineering Development Center (DYFS) Air Force Systems Command Arnold Air Force Station, Tennessee 37389		12. REPORT DATE June 1977 13. NUMBER OF PAGES 92
14. MONITORING AGENCY NAME & ADDRESS(if different from Controlling Office)		15. SECURITY CLASS. (of this report) UNCLASSIFIED 15a. DECLASSIFICATION/DOWNGRADING SCHEDULE N/A

16. DISTRIBUTION STATEMENT (of this Report)

Approved for public release; distribution unlimited.

17. DISTRIBUTION STATEMENT (of the abstract entered in Block 20, if different from Report)

18. SUPPLEMENTARY NOTES

Available in DDC

19. KEY WORDS (Continue on reverse side if necessary and identify by block number)

compressible flow
finite-difference methods
interaction methods
separated flow
computer programs
integral methods
turbulent boundary layers
transonic flow
inviscid flow

20. ABSTRACT (Continue on reverse side if necessary and identify by block number)

A computer code for a turbulent boundary-layer, inviscid interaction method for axisymmetric configurations of the type used for isolated nozzle afterbody models is presented. The method is applicable to flows with subsonic free streams, including slightly supercritical flows. The method consists of an integral boundary-layer method and a finite-difference inviscid-flow method which are coupled iteratively through the boundary-layer displacement thickness. Both attached and separated boundary layers can be

20. ABSTRACT (Continued)

calculated. An option is provided for calculating two-dimensional boundary layers. The procedure for separated flows is to specify the displacement thickness of the boundary layer and calculate the free-stream velocity distribution from both the boundary-layer equations and the inviscid-flow equations. The separation point location and the angle of the displacement surface are found by an iterative procedure. The equations programmed are presented along with detailed instructions for the preparation of input data, description of the program output and instructions for operation of the program on an IBM 370 computer. Sample cases are provided for a complete axisymmetric interaction calculation and for a two-dimensional boundary-layer calculation.

AFSC
Arnold AFS Tenn

PREFACE

The results reported herein were developed for the Arnold Engineering Development Center by Nielson Engineering and Research, Inc. under Contract F40600-76-C-0009. The author of this report was Gary D. Kuhn. The Air Force Project Engineer for this contract was E. R. Thompson, AEDC/DYR. The Program Element Number was 65807F. This report covers the work done during the period 15 March 1976 to 15 April 1977. The reproducibles used in the reproduction of this report were provided by the author.

CONTENTS

TABLES

ILLUSTRATIONS

1.0 INTRODUCTION

One of the critical areas in the design of both aircraft and missiles is the interaction between propulsive jets and the external flow over the aerodynamic shapes from which they issue. The drag of the afterbody and exhaust nozzle can be a significant fraction of the total vehicle drag. In order to obtain knowledge of the afterbody and nozzle flow fields and their interaction as early as possible in the design procedure, it is desirable to have a computational method for accounting for the viscous flow over the afterbody including separation and reattachment of the flow. Such a method should also account for the interaction between external inviscid flow over the afterbody and the viscous afterbody flow (including separated boundary layers).

This report describes a method for predicting the viscous flow field about an axisymmetric body at zero angle of attack. The method combines a finite-difference, inviscid-flow method with an integral boundary-layer method. The major difficulties in extending existing boundary-layer technology to flow on axisymmetric afterbodies are the same as those encountered in two-dimensional flows. First, a model for the turbulent Reynolds stresses must be employed. For the kind of bodies of interest herein, an eddy-viscosity model has been found which adequately accounts for the Reynolds stresses. For afterbody-nozzle configurations, the effect of the jet plume, boundary-layer, inviscid-flow interaction is also of major importance. Accounting for this interaction is a difficult problem. In the work described herein, the jet plume is simulated by a

solid body. Thus, the boundary-layer calculation involves separation on the boattail section of the afterbody with subsequent reattachment on the simulated plume.

The remainder of this report describes briefly the equations which are the basis of the calculative method and the particular technique used to calculate the viscous-inviscid interaction. Then the computer programs are described, followed by detailed instructions for the use of the programs. The composite computer program described herein contains the boundary-layer program developed for this work and an inviscid-flow program which is essentially the same as that described in reference 1. Both programs are incorporated as subprograms into a mainline program which performs an iteration to calculate the interaction between the boundary layer and inviscid flow for axisymmetric bodies of the type used for nozzle boattails followed by a solid plume simulator. The programs are written in the FORTRAN programming language for use on an IBM 370 computer. The boundary-layer program retains the capability to calculate two-dimensional flows as an option. Both the boundary-layer program and the inviscid-flow program can be used individually, without iterating if so desired.

2.0 DEVELOPMENT OF BOUNDARY-LAYER METHOD

The complete derivation of the governing equations for the boundary layer has been presented in reference 2. In this report the derivation is summarized and modified for the application of interest herein.

2.1 ASSUMPTIONS

The analysis is based on the following assumptions:

1. The governing equations are those for a compressible turbulent boundary layer.

2. The air behaves as an ideal gas.

3. The molecular viscosity, μ, is proportional to the temperature.

4. The specific heat of the gas is constant.

5. The wall is either two dimensional or axisymmetric, but can have arbitrary profile in the direction of flow as long as the longitudinal radius of curvature of the wall is large compared to the boundary layer.

6. The pressure is constant normal to the wall.

7. The wall temperature is constant.

2.2 BOUNDARY-LAYER EQUATIONS FOR COMPRESSIBLE TURBULENT FLOW

The basic notation and coordinate scheme are shown in figure 1. Note that the same symbols are used for the physical coordinates of both two-dimensional and axisymmetric configurations. Thus, r denotes the distance of a point from the axis of an axisymmetric configuration, or from the reference plane of a two-dimensional configuration, x is the distance along the axis, or reference plane measured from the leading edge, and the dimension y is measured from the body surface normal to the axis.

The governing equations describing the steady flow of a compressible turbulent boundary layer for both two-dimensional and axisymmetric configurations are:

Continuity

$$\frac{\partial}{\partial x}\left(r^k \rho u\right) + \frac{\partial}{\partial y}\left[r^k \rho (v - r_w' u)\right] = 0 \qquad (1)$$

Momentum

$$\rho u \frac{\partial u}{\partial x} + \rho (v - r_w' u) \frac{\partial u}{\partial y} = -\frac{dp}{dx} + \frac{1}{r^k}\frac{\partial}{\partial y}\left(r^k \mu\beta \frac{\partial u}{\partial y}\right) \qquad (2)$$

Energy

$$\rho u \frac{\partial S}{\partial x} + \rho (v - r_w' u) \frac{\partial S}{\partial y} = \frac{1}{r^k} \frac{\partial}{\partial y} \left[r^k \left\{ \mu \left[\frac{1}{P} + \frac{1}{P_T} (\beta - 1) \right] \frac{\partial S}{\partial y} \right. \right.$$

$$\left. \left. + \mu \left[\beta \left(1 - \frac{1}{P_T} \right) + \frac{1}{P_T} - \frac{1}{P} \right] \frac{u}{H_e} \frac{\partial u}{\partial y} \right\} \right] \tag{3}$$

where $k = 0$ for two-dimensional flow and $k = 1$ for axisymmetric flow, r_w' is the derivative of the body radius with respect to x, and

$$S = \frac{T_t}{T_{t_e}} - 1 \tag{4}$$

Equations (1), (2), and (3) are easily applicable to laminar and transitional flow. In laminar flow, substitution of $\beta = P_T = 1$ reduces the equations to those for a laminar boundary layer. Further, suitable variation of the eddy viscosity and turbulent Prandtl number makes the equations applicable to the transition region.

The boundary conditions for this system of equations are:

$y = 0$:

$$u = v = 0$$

$$r = r_w$$

$$S = S_w$$

$y = \infty$:

$$u = u_e(x)$$

$$\partial u/\partial y = 0$$

$$v = v_e(x)$$

$$S = 0$$

$x = x_o$:

$$u = u_o(y)$$

$$S = S_o(y)$$

2.3 TRANSFORMATION OF AXISYMMETRIC BOUNDARY-LAYER EQUATIONS TO ALMOST TWO-DIMENSIONAL FORM

In order to put the axisymmetric equations ($k = 1$) into a more convenient form, the Probstein-Elliott transformation (ref. 3) is applied. The coordinates of the axisymmetric body are shown in figure 1. The Probstein-Elliott transformation is

$$d\tilde{x} = \left[\frac{r_w(x)}{L}\right]^2 dx \tag{5}$$

$$d\tilde{y} = \frac{r(x,y)}{L}\, dy \tag{6}$$

where $r_w(x)$ is specified by the body shape and $r(x,y)$ is given by

$$r(x,y) = r_w(x) + y \tag{7}$$

The transformed continuity equation has the form

$$\frac{\partial(\rho\tilde{u})}{\partial\tilde{x}} + \frac{\partial(\rho\tilde{v})}{\partial\tilde{y}} = 0 \tag{8}$$

where

$$\rho\tilde{u} = \rho u \tag{9}$$

and

$$\rho\tilde{v} = -\frac{\partial\tilde{\psi}}{\partial\tilde{x}} = \frac{rL}{r_w^2}\,\rho(v - r_w' u) + \frac{L^2}{r_w^2}\frac{\partial\tilde{y}}{\partial x}\,\rho u \tag{10}$$

Applying the transformation to the momentum and energy equations (2) and (3) yields the transformed equations

$$\rho\tilde{u}\frac{\partial\tilde{u}}{\partial\tilde{x}} + \rho\tilde{v}\frac{\partial\tilde{u}}{\partial\tilde{y}} = -\frac{dp}{d\tilde{x}} + \frac{\partial}{\partial\tilde{y}}\left[(1 + kt\tilde{y})\mu\beta\frac{\partial\tilde{u}}{\partial\tilde{y}}\right] \tag{11}$$

$$\rho\tilde{u}\frac{\partial S}{\partial \tilde{x}} + \rho\tilde{v}\frac{\partial S}{\partial \tilde{y}} = \frac{\partial}{\partial \tilde{y}}\left[(1 + kt\tilde{y})\left(\mu A \frac{\partial S}{\partial \tilde{y}} + \mu \frac{B}{H_e}\tilde{u}\frac{\partial \tilde{u}}{\partial \tilde{y}}\right)\right] \tag{12}$$

where

$$A = \frac{1}{P} - \frac{1}{P_T} + \frac{\beta}{P_T} \tag{13}$$

$$B = \beta - \frac{\beta}{P_T} + \frac{1}{P_T} - \frac{1}{P} \tag{14}$$

and t is the transverse curvature factor

$$t = \frac{2L}{r_w^2} \tag{15}$$

and, from equations (6) and (7),

$$\tilde{y} = \frac{r_w}{L} y + \frac{1}{2L} y^2 \tag{16}$$

For flows in which the transverse curvature terms are negligible, letting $k = 0$ in equations (11) and (12) produces the equations of a two-dimensional boundary layer. The transverse curvature terms may be negligible for an axisymmetric flow if the body radius is large compared to the boundary-layer thickness. The Probstein-Elliott transformation is thus a first-order correction of the approximate equations for the effect of transverse curvature, allowing the boundary-layer thickness to be of the same order as the body radius.

2.4 TRANSFORMATION OF THE COMPRESSIBLE BOUNDARY-LAYER EQUATIONS

In order to simplify further the equations, the Stewartson transformation (ref. 4) reduces the equations to a set of equations for an incompressible flow. The following analysis is presented in terms of the Probstein-Elliott coordinates, $\tilde{x}$ and $\tilde{y}$, with the understanding that in the two-dimensional case $x = \tilde{x}$ and $y = \tilde{y}$.

In the Stewartson transformation the following variables are introduced:

$$X = \int_0^{\tilde{x}} \frac{p_e a_e}{p_{e_o} a_{e_o}} d\tilde{x} \qquad Y = \int_0^{\tilde{y}} \frac{\rho_e a_e}{\rho_{e_o} a_{e_o}} \frac{\rho}{\rho_e} d\tilde{y} \tag{17}$$

$$U = \frac{a_{e_o}}{a_e} \tilde{u} \tag{18}$$

$$V = \frac{p_{e_o}}{p_e}\left(\frac{a_{e_o}}{a_e}\right)^2 \tilde{u} \frac{\partial}{\partial \tilde{x}} \int_0^{\tilde{y}} \frac{\rho_e a_e}{\rho_{e_o} a_{e_o}} \frac{\rho}{\rho_e} d\tilde{y} + \frac{p_{e_o} a_{e_o}}{p_e a_e} \frac{\rho}{\rho_{e_o}} \tilde{v} \tag{19}$$

With these the boundary conditions become:

$\tilde{y} = 0$: $\quad U = V = 0$

$\quad S = S_w$

$\tilde{y} = \infty$: $\quad U = U_e = a_{e_o} M_e$

$\quad \partial U/\partial Y = 0$

$\quad S = 0$

It is assumed that S and the eddy-viscosity parameter, β, transform directly; that is,

$$S(X,Y) = S(\tilde{x},\tilde{y}) \tag{20}$$

$$\beta(X,Y) = \beta(\tilde{x},\tilde{y}) \tag{21}$$

It is easily shown, using relations (17) through (21) and the perfect gas assumption along with the relations

$$\frac{\mu}{\mu_{e_o}} = C \frac{T}{T_{e_o}} \tag{22}$$

and

$$\frac{\partial p}{\partial y} = 0 \tag{23}$$

that the boundary-layer equations in the Stewartson plane are:

<u>Continuity</u>

$$\frac{\partial U}{\partial X} + \frac{\partial V}{\partial Y} = 0 \tag{24}$$

<u>Momentum</u>

$$U \frac{\partial U}{\partial X} + V \frac{\partial U}{\partial Y} = (S+1) U_e \frac{dU_e}{dX} + C\nu_{e_o} \frac{\partial}{\partial Y}\left[(1 + kt\tilde{y})\beta \frac{\partial U}{\partial Y}\right] \tag{25}$$

<u>Energy</u>

$$U \frac{\partial S}{\partial X} + V \frac{\partial S}{\partial Y} = C\nu_{e_o} \frac{\partial}{\partial Y}\left[(1 + kt\tilde{y}) A \frac{\partial S}{\partial Y}\right]$$

$$+ C \frac{\nu_{e_o}}{H_e} \frac{a_e^2}{a_{e_o}^2} \frac{\partial}{\partial Y}\left[(1 + kt\tilde{y}) BU \frac{\partial U}{\partial Y}\right] \tag{26}$$

The coordinate $\tilde{y}$ is not transformed in the transverse curvature terms because integration of the equations across the boundary layer is anticipated and only corresponding values are needed in those terms. The Chapman-Rubesin parameter, C, is assumed to be at most a function of x. In the work presented herein, C is a constant evaluated at the wall temperature; that is,

$$C = \frac{\mu_w}{\mu_{e_o}} \frac{T_{e_o}}{T_w} = \left(\frac{T_w}{T_{e_o}}\right)^{1/2} \left(\frac{T_{e_o} + T_s}{T_w + T_s}\right) \tag{27}$$

where Sutherland's law is used to evaluate the viscosity.

$$\mu = \lambda \frac{T^{3/2}}{T + T_s} \tag{28}$$

where λ and T_s are constants.

In the remainder of this report, the solution of the energy equation (26) will be approximated by the Crocco relation

$$S = S_w\left(1 - \frac{U}{U_e}\right) \tag{29}$$

Thus, the velocity profiles found to be valid for incompressible, two-dimensional turbulent boundary layers can be used by simply transforming the input quantities to the incompressible plane, performing the calculation for an equivalent incompressible boundary layer, and then transforming the results back to the compressible plane, and for an axisymmetric flow, back to the axisymmetric coordinates.

2.5 DEVELOPMENT OF INTEGRAL BOUNDARY-LAYER METHOD

2.5.1 Integral Equations

The integral method used herein was described in detail in reference 5. Families of integral equations are derived by eliminating V between the momentum and continuity equations and then taking weighted integrals of the resulting equation across the boundary layer.

$$\int_0^{\delta_i}\left[UU_X - U_Y \int_0^Y U_X d\eta - (S+1)U_e(U_e)_X - \nu(\beta U_Y)_Y\right]f(Y)\,dY = 0 \tag{30}$$

In the present case, the functions

$$f = Y^n\ ; \quad n = 0,1 \tag{31}$$

produce the momentum and moment of momentum integral equations, respectively.

2.5.2 Velocity Profiles

The Y dependence of the integral equations is eliminated by substituting an appropriate parametric formulation for the velocity profiles. The function used for the present theory is a modification of Coles' family (ref. 6) with a laminar sublayer added and the wake function approximated analytically.

$$U = U_\tau[2.5\ln(1+Y^+) + 5.1 - (3.39Y^+ + 5.1)\exp(-0.37Y^+)] + U_\beta \sin^2\left(\frac{\pi}{2}\right)\frac{Y}{\delta_i} \tag{32}$$

The parameter U_τ is the friction velocity,

$$U_\tau = \frac{C_f}{|C_f|} U_e \sqrt{\frac{C_f}{2}} \tag{33}$$

The variable Y^+ is defined to account for the axisymmetry of the flow

$$Y^+ = \frac{|U_\tau| Y}{\nu_{e_o}} \left(\frac{L}{r_w}\right)^k \tag{34}$$

The other parameters in equation (32) are δ_i, the boundary-layer thickness and U_β a wake velocity. The exponential terms and the additional unit in the logarithmic term provide a smooth transition from the turbulent flow to the wall through a laminar sublayer.

2.5.3 Eddy Viscosity

The eddy-viscosity model used in this work is an extension of the two-layer model used by Kuhn (ref. 2) including an

intermittency function for the outer layer and a modification of the outer layer for adverse pressure gradients and separated flows. In the inner layer of attached flows, the eddy-viscosity parameter, β, is represented by an exponential expression based on the law of the wall. In the outer layer Clauser's expression, modified for adverse pressure gradients, is used along with an intermittency function giving

$$\beta = [0.013 + 0.0038 \exp(-\delta_K^* p_X/15\tau_w)] U_e \delta_K^* / [1 + 5.5(\tilde{y}/\delta)^6] \qquad (35)$$

For favorable pressure gradients, the exponential term in equation (35) is taken to be unity.

For separated flows, the eddy viscosity across the entire layer is represented by a relation based on the velocity profile above the $U = 0$ line.

$$\beta = 0.013[1 + 5.5(\tilde{y}/\delta)^6]^{-1} \frac{U_e}{\nu} \int_{y_{u=0}}^{\delta} \left(1 - \frac{U}{U_e}\right) dy \qquad (36)$$

2.5.4 Transitional Eddy Viscosity

Transition from laminar to turbulent flow is calculated by letting the eddy viscosity change from a laminar viscosity to a fully turbulent value over a short distance according to the relation

$$\beta_t = [1 - \exp(-K(x - x_t)^2)](\beta_T - 1) + 1 \qquad (37)$$

where

β_t is the transitional eddy viscosity

β_T is the turbulent eddy viscosity

x_t is the location of the beginning of transition

and

$$K = \frac{0.0001}{\delta_t^2}$$

where

δ_t is the boundary-layer thickness at x_t.

2.5.5 Equations Solved

Substitution of equation (32) into the two equations produced by equations (30) and (31) produces two ordinary differential equations for the variation of the variables U_τ, U_β, δ_i, and U_e with x. A third equation produced by evaluating equation (32) at $Y = \delta_i$ allows the elimination of U_β from the equations, leaving a set of two equations

$$A_{11}(U_\tau)_x + A_{12}\delta_{i_x} + A_{13}(U_e)_x = -U_\tau|U_\tau|/U_e\delta_i \tag{38}$$

$$A_{21}(U_\tau)_x + A_{22}\delta_{i_x} + A_{23}(U_e)_x = -\frac{\nu}{U_e\delta_i^2}\int_0^{\delta_i} \beta U_Y \, dY \tag{39}$$

Anticipating the development of a viscous-inviscid interaction, the velocity, U_e, is considered to be a dependent variable. The coefficients A_{ij} are functions of the variables U_τ, δ_i, and U_e. The usual procedure for solving equations (38) and (39) for attached boundary layers is to prescribe the pressure distribution or the free-stream velocity distribution, U_e. However, if separation occurs, the pressure distribution cannot be prescribed arbitrarily in the separated region. If an adverse pressure gradient is prescribed for an attached boundary layer, the value of U_τ can approach zero. When U_τ vanishes, the coefficients A_{11} and A_{22} in equations (38) and (39) also vanish, producing a singularity. The singularity can be removed by rearranging the equations so that U_τ is not

a dependent variable. One method of accomplishing this is simply to rearrange the equations so that U_τ can be prescribed and U_e can be calculated as a dependent variable as shown in reference 7.

Another method of avoiding the singularity at $U_\tau = 0$ is used in the method described herein. The displacement thickness, δ^*, is expressed in terms of U_τ, δ_i, and U_e and the result is differentiated with respect to x, producing a third equation.

$$A_{31}(U_\tau)_x + A_{32}\delta_{i_x} + A_{33}(U_e)_x + U_e\delta^*_x = 0 \tag{40}$$

where the A_{3i} are functions of U_τ, δ_i, and U_e and A_{31} vanishes when $U_\tau = 0$. It can be shown that A_{11}/A_{31} and A_{21}/A_{31} are both finite when $U_\tau = 0$. This allows the three equations, (38), (39), and (40), to be reduced to two ordinary differential equations in the four dependent variables, U_τ, δ^*, δ_i, and U_e. The resulting equations are:

$$\frac{A_{11}}{A_{31}} U_e\delta^*_x + \left(\frac{A_{11}}{A_{31}} A_{32} - A_{12}\right)\delta_{i_x} + \left(\frac{A_{11}}{A_{31}} A_{33} - A_{13}\right)(U_e)_x = \frac{U_\tau|U_\tau|}{U_e\delta_i} \tag{41}$$

$$\frac{A_{21}}{A_{31}} U_e\delta^*_x + \left(\frac{A_{21}}{A_{31}} A_{32} - A_{22}\right)\delta_{i_x} + \left(\frac{A_{21}}{A_{31}} A_{33} - A_{23}\right)(U_e)_x = \frac{\nu}{U_e\delta_i^2}\int_0^{\delta_i} \beta U_Y dY \tag{42}$$

The value of U_τ can be obtained directly from known values of δ^*, δ_i, and U_e by solving the nonlinear relation

$$\delta^* = f(U_\tau, \delta_i, U_e) \tag{43}$$

Prescribing the distribution of δ^* in equations (41) and (42) and obtaining U_τ from equation (43) is equivalent to prescribing U_τ as described previously.

2.5.6 Method of Solution of Equations

The equations (38) and (39), or (41) and (42) are integrated numerically using a fourth-order Adams-Moulton predictor-corrector integration with a fourth-order Runge-Kutta scheme used to obtain starting values. By doubling or halving the integration step size, the integration is capable of some optimization of the integration. Thus, numerical errors are kept within certain bounds by dividing the integration step by 2 whenever the error is too large and multiplying the interval by 2 whenever less accuracy is necessary than is being obtained. The step size is allowed to decrease to as small a value as 10^{-6} before the calculation is terminated.

3.0 INVISCID-FLOW MODEL

The inviscid-flow method employed herein is the finite-difference solution of the full potential equation described in references 1 and 8. The computer program used is that described in reference 1 with minor modifications to accommodate the iteration between the inviscid and boundary-layer flows. The detailed derivation of the flow equations, the calculative method, and the computer program are contained in references 1 and 8 and will not be repeated here. A general description of the program is summarized here from reference 1.

"One of the important considerations when trying to solve the full potential equation is the choice of a coordinate system. For complex three-dimensional shapes cartesian coordinates may be best; however, for simpler two-dimensional or axisymmetric shapes the use of a coordinate transformation such that the

body lies along a coordinate line can greatly simplify the application of the exact boundary condition at the body surface. The program described in this paper uses a body-normal coordinate system for closed bodies. For open bodies (i.e., bodies with a sting or simulated wake) it uses a body-normal system on the forebody up to the first horizontal tangent and a sheared cylindrical coordinate system aft of that point. This coordinate system is suitable for closed bodies which are blunt on both ends and convex and smooth over the entire body or for open bodies which are blunt-nosed and convex and smooth up to the first horizontal tangent. It is possible to treat pointed bodies and bodies with slope discontinuities but the coordinate system is not well suited for them and their solution may not be as accurate as the blunt-body solutions."

"A stretching is applied to both the normal and tangential coordinates such that the infinite physical space is mapped to a finite computational space. Thus, the boundary condition at infinity can be applied directly and there is no need for an asymptotic far-field solution. Details about the stretching functions are given in [reference 1] appendix A."

"The general method of solution is to replace the governing second-order partial differential equation with a system of finite-difference equations, including Jameson's rotated difference scheme at supersonic points. The difference equations are solved by a column relaxation method."

"The boundary condition at the body surface is applied through the use of dummy points inside the body. Details of this computation are given in [reference 1] appendix B."

4.0 VISCOUS-INVISCID INTERACTION METHOD

Separation is the result of an adverse pressure gradient causing reversal of the low-energy, low-momentum fluid near the wall in the boundary layer. The adverse pressure gradient is determined by the inviscid flow field and is the net result of the body shape and the displacement effect of the boundary layer. Thus, the viscous and inviscid flow fields are interdependent. Accounting for this interdependence with an interaction model is made difficult by the fact that the boundary-layer equations are parabolic and therefore cannot respond to disturbances downstream of local stations, while for subsonic and transonic flows the inviscid flow is elliptical and therefore subject to influence by the entire flow field. In the method described herein, the boundary-layer and inviscid-flow methods are used alternately in an iterative scheme.

Before proceeding with the description of the iterative scheme developed in the work, it is worthwhile to consider two important results. The work of Presz (ref. 9) has shown that the displacement effect of the separated boundary layer on an afterbody can be represented by a conical surface placed between the separation and reattachment points. Reubush and Putnam (ref. 10) went a step further, and devised a calculative scheme in which the conical surface was treated as a solid surface and the boundary layer was calculated on the modified body. No reversed flow was calculated and the separation prediction method used in that work was based only on the inviscid pressure distribution calculated for the real body alone and thus could not account for Reynolds number effects. Nevertheless, these methods reveal significant information about the nature of the boundary layer in the region of strong interaction. First, the boundary layer grows smoothly as it encounters the adverse pressure gradient, and second the displacement surface assumes

a condition such that its effect after separation can be approximated by a conical surface.

4.1 ESTIMATION OF SEPARATION POINT LOCATION

The first step in calculating the viscous-inviscid interaction is to calculate the inviscid flow over the plain body. The resulting distribution of the velocity at the boundary, u_e, is then prescribed for the boundary-layer calculation using equations (38) and (39). If strong adverse pressure gradients exist, the boundary-layer calculation may reach a point where the skin-friction coefficient approaches zero and the numerical calculation can proceed no further with u_e prescribed. This point is not necessarily the true location of separation, however, since the interaction with the inviscid flow has not yet been accounted for.

A better first approximation to the location of separation x_s can be found by computing the shape factor, H_{tr}.

$$H_{tr} = \frac{\int_0^{\delta_i} \left(1 - \frac{U}{U_e}\right) dY}{\int_0^{\delta_i} \frac{U}{U_e}\left(1 - \frac{U}{U_e}\right) dY} \tag{44}$$

For the velocity profiles given by equation (32) this parameter has a value of 4.0 when $U_\tau = 0$. However, experimental measurements indicate that separation actually occurs when H_{tr} is approximately 2.0. This suggests that the present boundary-layer approximation is not accurate in the vicinity of the separation point. The major cause of the inaccuracy is believed to be the neglect of any upstream influence of the separated region inside the boundary layer. However, the effect of the separated region which is transmitted upstream in the boundary

layer is believed to be small compared to the effect transmitted through the inviscid flow. In this work, the first approximation to the value of x_s is the location at which $H_{tr} = 1.5$ for the inviscid velocity calculated for the plain body.

4.2 ESTIMATION OF BOUNDARY OF SEPARATED REGION

At the separation point, x_s, the skin friction is assumed to have become zero and the calculation is carried on into the separated flow using a prescribed distribution of δ^* with equations (41) to (43). The result of that calculation is a solution for the free-stream velocity (the "viscous velocity") which may or may not agree with the "inviscid velocity" produced by calculating the inviscid-flow theory. An iterative procedure is used to find the particular variation of δ^* downstream of x_s for which the "viscous velocity" and the "inviscid velocity" agree.

A two-parameter analytical formulation is used to represent the effective displacement surface between separation and a point downstream of reattachment. Thus, the effective body shape is given by

$$r = r_w + \delta^* \quad \text{for} \quad 0 < x < x_s \quad \text{and} \quad x_p < x < \infty \tag{45}$$

$$r = (r_w + \delta^*)_s + (x - x_s)\tan\theta_s \quad \text{for} \quad x_s < x < x_p \tag{46}$$

where x_p is the location of the peak inviscid pressure as given by the previous inviscid solution and θ_s is the angle of the extrapolated δ^* surface with the axis.

A first approximation to the angle, θ_s, is obtained from an expression presented in reference 10.

$$\theta_s = \tan^{-1}\left(\frac{dr_w}{dx}\right) + 14.4 - 4.89\ M_s \tag{47}$$

Downstream of x_p the free-stream velocity is again prescribed on the boundary layer (eqs. (38) and (39)) as an exponential fairing between the value at x_p and the inviscid velocity from the previous calculation.

4.3 ITERATION PROCEDURE

The method developed in this work consists of three iterations. One iteration is used to locate the separation point, x_s. Another iteration is used to determine the angle, θ_s, of a conical displacement surface. The third iteration calculates the best solution for specific values of x_s and θ_s. The iteration procedure is described schematically in figure 2.

The iteration procedure consists of three cycles. In the inner cycle, the inviscid flow and the boundary layer are calculated alternately until the largest change in the δ^* solution between iterations becomes smaller than a specified percent. At each step of the cycle, the boundary-layer displacement thickness is used to calculate an augmented body shape by the relation

$$r_n = r_w + \alpha\delta_n^* + (1 - \alpha)\delta_{n-1}^* \tag{48}$$

where r_n is the effective body radius at iteration n and α is a damping factor, usually equal to 0.5.

When the inner cycle has been terminated, the calculation is complete if no separation occurred. However, if separation is present, there exist two solutions for the free-stream velocity as described previously. The next step of the procedure is to calculate the squared deviation between the two solutions downstream of x_s at 19 points.

$$s = \sum_{1}^{19} (u_{e_V} - u_{e_I})^2/u_{e_o}^2 \tag{49}$$

where u_{e_V} is the "viscous velocity" and u_{e_I} is the "inviscid velocity." This quantity is then compared with the value from the previous θ_s iteration and if a minimum has not been found, θ_s is adjusted in an appropriate manner, the boundary layer is recalculated using the new value of θ_s and the calculation reenters the inner cycle. This process is repeated until a minimum of the squared deviation, s, is found. The present program calculates the best fit for changes in θ_s within 0.5°.

When the θ_s cycle is complete, for a given value of x_s, the next step is to adjust x_s in an appropriate manner and reenter the θ_s cycle. These cycles are repeated until the smallest value of s is found, establishing θ_s within 0.5° and x_s within a distance equal to the value of δ^* at x_s.

An alternate termination device is incorporated in the computer program to aid in keeping the cost of the solution at a minimum. If the squared deviation, s, is smaller than 0.0005 at any step of the iteration, the iteration procedure terminates.

5.0 COMPUTER PROGRAM ORGANIZATION

In this section, the general organization of the programs will be described. Specific information on data required for input and data developed for output will be described in sections 6, 7, and 8. Sample Job Control Card decks for a typical IBM 370 installation are presented in section 9.

The overall program consists of a mainline program (program 1) and two main subprograms each consisting of several subroutines. The first main subprogram is the inviscid-flow program (program 2). It is a modified version of the

program described in reference 1. The second main subprogram is the boundary-layer program (program 3). It is based on the integral theory described previously and retains the two-dimensional case as an option. The mainline program controls the iteration between the other two programs. Either of the two subprograms may be used separately, without iterating by appropriate choice of the input parameters.

Both the boundary-layer program and the inviscid-flow program require some punched card input and some input data from disc or tape data files. The data files must be identified by specific Logical Unit numbers. Each program in turn produces new data files and printed output. The general relationship of the programs and the various data files are shown in figure 3. The specific Logical Unit numbers required for input and output are listed in Table I. Two Logical Unit numbers are associated with each data file shown in figure 3. One unit is used for input, the other for output.

Program 2 requires initially data from cards describing the free-stream conditions, the computational mesh and the body shape. Alternately, the program can accept the input body shape from data file 1. It can also accept an initial solution for the perturbation velocity potential from another data file (data file 2). Program 2 produces printed output lists of the appropriate flow field quantities, quantities describing the configurations and the computational mesh and several data files. Data file 2 is rewritten using the new solution for the potential. A third file (data file 3) is written containing the distribution of the axial velocity component for use by the boundary-layer program.

Program 3 requires initially the free-stream conditions and gas constants as well as parameters describing the shape of the surface over which the boundary layer is flowing. On the first iteration of a viscous-inviscid interaction, the surface shape

is the same as that for program 2. On subsequent iterations, the body shape for the boundary-layer program remains the same while that for the inviscid flow is modified by the addition of the boundary layer. Program 3 can also accept data from data files as optional input. The free-stream velocity distribution, u_e, can be input from data file 3, produced by program 2. The distribution of the body shape augmented by the displacement thickness can be input from data file 4. That file differs from data file 1 because it contains the raw data for $\delta^* + r_w$ versus x as calculated by the boundary-layer program while data file 1 contains the shape adjusted according to equation (48) and interpolated to the x stations of the original input shape. If program 3 is being used separately from program 2 (i.e., without iterating), two additional options are available for card input. Either the free-stream velocity, u_e, can be input as mentioned previously, or the displacement thickness, δ^*, may be input. These options are described more fully in sections 6.2 and 7.1.

Program 3 produces as output lists of the boundary layer and flow quantities as they are calculated along the body. In addition, program 3 produces an updated version of data file 4 and the augmented body shape (data file 1) required by program 2. Data file 4 also contains a list of the velocity ratio u_e/u_{e_o} corresponding to the boundary layer.

Program 3 can be used in a two-dimensional mode if desired. However, calculation of a viscous-inviscid interaction can only be done for axisymmetric cases with the present inviscid program.

All card input pertaining to programs 2 and 3 is input through program 1. Program 1 also produces a file of the quantities needed to restart the calculation if the calculation should terminate before all iterations are completed. These data are stored on data file 5. Detailed instructions regarding restarting are presented in section 7.3.

6.0 INPUT TO THE PROGRAMS

The data required by the programs generally fall into three categories: (1) geometrical data; (2) flow field data; and (3) control parameters. The control parameters are indices for specifying options and iteration counters. It will be noted by comparison with reference 1 that a number of input quantities required for the inviscid-flow program have been eliminated in the present version. This has been done by incorporating the calculations required to obtain some of the quantities into the present code or by simply defining fixed values which have been found to be successful. Specifically, a value of 1.4 is used for the initial value of the subsonic relaxation factor, a value of 0.1 is used for the initial value of the supersonic relaxation factor and a value of 1.3 is used for the exponent in the normal coordinate stretching function. Also, it is assumed that the computational grid has equal step sizes in both coordinate directions at the nose of the body.

The general requirement of the input data is that the tabular lists of the various distributions required represent smooth curves. This is especially true of the list of body shape coordinates. The inviscid program uses cubic splines to fit the input coordinates, so those coordinates must accurately represent a smooth curve with continuous second derivatives.

6.1 TABULAR FORM

The input data required for calculating transonic boundary-layer, inviscid-flow interactions consist of several punched cards containing parameters describing the free-stream flow conditions, the computational mesh for the inviscid calculation, initial values for the boundary-layer calculation, and certain options that are available in the programs. A dictionary of the input data is presented in the next section. Table II shows

the input variables as they are to be punched on the data cards. More detailed explanation of the requirements for the inviscid-flow program are presented in reference 1 and are not repeated herein.

6.2 DICTIONARY OF INPUT VARIABLES

The variables required for input on punched cards are defined in this section in the order in which they are required. Additional details on the format of the punched data are given in Table II. The first three cards of any input data deck contain a description of the case being calculated. Any or all of these three cards may be blank, but all three are required. The remaining variables in Table II are as follows:

LPROG Integer indicating level of calculation.

- = -1 Inviscid flow only.
- = 0 Inviscid-viscous interaction.
- = 1 Boundary layer only.

NRSTRT Integer indicating whether calculation is being restarted to continue a previous calculation. Only needed if LPROG = 0.

- = 0 Start from zero. Input all quantities on cards or data files as required.
- > 0 Restart. Input data file 5 (Logical Unit 11) containing data from previous iteration plus all other input data files.

NPRINT Integer indicating quantity of output to be printed (see section 8.1).

- = 0 Minimum output.
- = 1 All output.

N1MAX Integer convergence criterion for inner iteration cycle. The cycle is considered to be converged when the maximum change in δ^* between iterations is less than N1MAX percent. A value of 7 is good for most

N1MAX (conc.)	engineering purposes. More accuracy is obtained with smaller values at increased cost. However, a maximum of 11 iterations will be performed in the inner cycle in any case.
N1	Integer iteration counter for inner viscid-inviscid iteration.
N2	Integer iteration counter for θ_s iteration presently limited to a maximum of 20.
N3	Integer iteration counter for x_s iteration presently limited to a maximum of 20.
IBL	Integer indicating how interaction calculations are to begin. = 3 Start with inviscid flow. = 0 Start with boundary layer.
MIT2	Integer number of iterations to be executed by the inviscid program in solving its relaxation equations for the first series of calculations in the inner iteration cycle. After the inner iteration cycle has been converged for the first time, the relaxation iteration limit is set equal to the value of MIT to be input subsequently. A typical value for MIT2 is 20 for interaction calculations. A larger value may be better for some transonic cases.
GAMMA	Ratio of specific heats.
AMINF	Free-stream Mach number.
IXY	Integer number of values of coordinate pairs, XO,YO, to be input for inviscid body shape. If IXY = 0, the required shape must be input from data file 1 (Logical Unit 14). Maximum value is 100.
XO,YO	Axial and radial coordinates of body shape for inviscid-flow calculation, 2 per card.

The next series of variables, items 6 and 7 in Table II, are for the inviscid-flow program. Detailed information on how these data are to be obtained is contained in reference 1.

IMAX Number of grid lines in the tangential direction; I = 1 is the forward stagnation line, I = IMAX is the rear stagnation line for closed bodies and downstream infinity for open bodies. For each grid refinement IMAX is increased such that $IMAX_{NEW} = 2(IMAX_{OLD}) - 1$. The present limit on IMAX is 81. Instructions for changing this limit appear as comments in the program listing (subroutine ONEO).

JMAX Number of grid lines in the normal direction; J = 1 corresponds to an infinite distance from the body and J = JMAX is on the body. The same formula and limit that apply to IMAX also apply to JMAX.

MIT Maximum number of iterations (complete relaxation cycles) allowed for the inviscid-flow program after complete inner cycle or when using the inviscid-flow program alone. A typical value for interaction calculations is same as MIT2. The values of MIT and MIT2 are combined for the final iteration of an interaction calculation so that a total of MIT+MIT2 relaxation cycles are performed.

MHALF Number of grid refinements to be done. For interaction calculations a value of zero should be used with a grid fine enough for adequate resolution.

KLOSE Body type.
= 0 Open body (i.e., one with a sting or wake).
= 1 Closed body.

NPLOT Plot trigger; NPLOT = 1 causes write on disc for input to plot routines and calling of plot routines. (The

plot routines are not included in the present version so NPLOT = 0 should be put in.)

LREADP Integer indicating whether initial estimate of potential distribution is to be input from data file 2 (Logical Unit 13).
= 0 - no
= 1 - yes

DETAO Step size of the normal coordinate at the body.

XIXM Value of the computational coordinate, X, at the matching point of the two stretching functions used in the finite-difference scheme (see ref. 1), for open bodies only. Since X varies from zero to one, XIXM is the fraction of the total number of grid points which will be in the first stretching region (ahead of x_m). Usual value is about 0.85. The exact value used should be chosen so that one grid point, usually the one at x_m, corresponds to the boattail-sting junction.

XM Axial location, x_m, (in physical coordinates) of the junction (or matching point) between the two tangential stretching functions, for open bodies only, see reference 1. Must be less than XO(IXY). This parameter is used to concentrate computational mesh points in a certain region. The usual approach for interaction calculations is to let x_m be equal to the length of the body to the beginning of the sting, XBT.

XIM1 Approximate location of the last finite value of the tangential coordinate for open bodies; usually about 2 or 3 maximum diameters larger than the length of the body, XBT.

XBT Length of the body to the beginning of the sting.

The remaining input variables are related to the boundary-layer program alone or to the viscous-inviscid interaction method.

XZNEW Axial location at which boundary-layer calculations will begin after four iterations have been calculated. The usual procedure is to start the boundary-layer calculations close to the nose of a long body at XZ (see item 15 in Table II) and then after four iterations move the starting point to XZNEW (XZNEW > XZ). In subsequent iterations, the boundary layer does not change for X < XZNEW. For long slender bodies with boattails, XZNEW can usually be near the beginning of the boattail.

DTHET Angular deviation of extraplated δ^* surface from the programmed value given by equation (47). Usual starting value is 0.0°.

LSEP Logical variable indicating whether the location of separation (XSEP) is known (.TRUE.) or not (FALSE).

XSEP Axial location of separation. Put in only if LSEP = TRUE.

IOPT Integer indicating the mode of the calculation.

= 1 u_e is to be input.

= 2 δ^* is to be input.

Put in a value of 1 for starting an interaction calculation.

K Integer indicating whether flow is axisymmetric.

= 0 Two dimensional.

= 1 Axisymmetric.

LVAR1 Integer indicator for method of input of u_e when IOPT = 1.

= 0 Input u_e (dimensional) on cards.

= 1 Input u_e/u_{e_o} on cards.

= 2 Input u_e/u_{e_o} from data file 3 on Logical Unit 12.

LSHAPE Integer indicating option for calculating all initial conditions (I.C.) except u_e (see section 7.4).

= 0 Input initial values per LIC.

= 1 Calculate I.C. for flat plate.

= 2 Calculate I.C. for cylinder.

= 3 Calculate I.C. for cone.

LIC Integer indicating initial condition options for IOPT = 1 and LSHAPE = 0.

= 1 Put in CFC1 and DELTA1.

= 2 Put in CFC1 and DELST1.

LDSTAR Integer indicating whether a file of $\delta^* + r_w$ is to be input.

= 0 No input.

= 1 File of $\delta^* + r_w$ versus x is required on Logical Unit 15 (data file 4).

IUNIT Integer indicating which value of the gas constant, RGAS, and the constants in Sutherlands temperature-viscosity relation (eq. (28)) are to be used. The choice depends on whether air is the gas being calculated and the units of the input quantities.

= 1 Input units must be pounds, feet, seconds, and ^oR.

= 2 Input units must be pounds, inches, seconds, and ^oR.

= 3 Input units must be newtons, meters, seconds, and ^oK.

For another gas, or other units, put in anything for IUNIT and put in nonzero values of VISC, RGAS, and SCON.

LSHPBL Integer indicating whether body shape is to be input for boundary-layer calculations.

= 0 XRL and RL are assumed to be the same as XO and YO. This is usually the case when starting an interaction calculation.

= 1 XRL and RL will be required.

NOTE: The next three variables, NVAR, XVAR, VAR, are only required on cards if LPROG = 1 and LVAR1 = 0 or 1.

NVAR — Integer indicating the number of values to be input for the prescribed variable (u_e or δ^*). Maximum value is 100.

XVAR, VAR — Axial location and value of prescribed variable as follows:

IOPT = 1 and LVAR1 = 0, VAR = u_e

IOPT = 1 and LVAR1 = 1, VAR = u_e/u_{e_o}

IOPT = 2, VAR = δ^*

EL — Reference length. Needed if input data lengths are nondimensionalized. If lengths are dimensional, put in EL = 1.0.

PT — Total pressure, p_t (lb/ft²), (lb/in²), or (newton/m²).

TT — Total temperature, T_t (°R) or (°K).

TWONTT — Ratio of body surface temperature to total temperature, T_w/T_t.

VISC — Constant λ in Sutherlands formula for viscosity, equation (28). If one of the programmed values is acceptable, put in a value of 0.0. The value used will then be determined by the value of IUNIT on item number 11 as follows:

IUNIT	VISC	
1	$2.27(10^{-8})$	lb sec/ft² $(^{o}R)^{1/2}$
2	$1.5764(10^{-10})$	lb sec/in $(^{o}R)^{1/2}$
3	$1.4582(10^{-6})$	Newton sec/m $(^{o}K)^{1/2}$

RGAS — Gas constant. If one of the programmed values is acceptable, put in a value of 0.0. The value used will be determined by the value of IUNIT as follows:

RGAS (conc.)

IUNIT	RGAS	
1	1716.0	ft^2/sec^2 ^oR
2	247104.0	in^2/sec^2 ^oR
3	286.96	m^2/sec^2 ^oK

SCON Constant T_s, in Sutherlands viscosity law, equation (28). If one of the programmed values is acceptable, put in a value of 0.0. The value used will be determined by the value of IUNIT as follows:

IUNIT	SCON	
1	198.6	^oR
2	198.6	^oR
3	110.333	^oK

DFACT Relaxation factor for adding δ^* to body, the factor α in equation (48). Usual value is 0.5. If a value of 0.0 is put in, a value of 0.5 will be used.

XZ Axial location of beginning of boundary-layer calculation.

RLEN Axial location of end of boundary-layer calculation. Usually at least one maximum diameter larger than XBT.

XT Axial location of transition from laminar to turbulent boundary-layer flow.

DXZ Integration step size at the beginning of the boundary-layer calculation. The usual procedure is to use a small value for a new case until experience indicates whether a larger value would work. If too large an initial step is attempted, the first step of the integration procedure may calculate a negative value of δ_i and the calculation will terminate. A typical value would be $(10^{-4})\cdot$XBT.

DXP Axial interval at which velocity profiles are to be printed. If a value of 0.0 is put in, no profiles are

DXP (conc.) printed. In any case, profiles will not be printed more often than the output step specified by DXOUT.

DXOUT Axial interval at which output of the local values of u_τ, δ, δ^*, θ, C_f, u_e/u_{e_o}, C_p, $\delta^* + r_w$, DX, and H_{tr} are to be printed. The output may be at irregular intervals since the output location is determined as the point where the local value of X first becomes greater than XOUT. The new value of XOUT is then calculated as XOUT = X + DXOUT. This value should be selected to produce less than 200 printed output steps for the entire length of the body.

HLIM Limit value of H_{tr} to indicate separation. Input of a blank or a value of 0.0 will cause a value of 1.5 to be used as discussed in section 4.1. If the interaction iteration has difficulty converging due to a very small separated region, it may be necessary to increase this value slightly in order to calculate a fully attached boundary layer. A value greater than 4.0 will allow the calculation to proceed to a singularity if one should occur. The calculation will terminate at that point.

CFC1 Value of skin-friction coefficient at initial boundary-layer station (see section 7.4).

DELTA1 Value of boundary-layer thickness, δ (compressible), at initial boundary-layer station (see section 7.4).

DELST1 Value of boundary-layer displacement thickness, δ^*, at initial boundary-layer station (see section 7.4).

UE1 Value of free-stream velocity at initial boundary-layer station.

DUEDX Value of free-stream velocity gradient at initial boundary-layer station.

NR Integer number of values of XRP and RL to be input for body shape. If NSHPBL = 0, this is assumed to be the same as IXY. Maximum value is 100.

XRP,RL Axial and radial coordinates of body shape for boundary-layer calculation. If LSHPBL = 0, these are assumed to be the same as XO and YO, respectively. For two-dimensional configurations, these represent the x and y coordinates of a surface measured from a reference plane.

7.0 PROGRAM OPTIONS

Several optional modes of calculation are available through the input parameters. A description of the options and the corresponding values of the pertinent parameters follows.

7.1 BOUNDARY-LAYER OPTION

To use only the boundary-layer program, put in the three card description, then the first value on the fourth input data card should be:

LPROG=1 (see Table II)

The remaining variables shown on item number 2 in Table II are not required. The remaining cards would be those corresponding to item 3 and items 11 to 19 as described in Table II. With this option, the user has the choice of specifying either the free-stream velocity, u_e, or the displacement thickness, δ^*, through the variables NVAR, XVAR, and VAR on items 12 and 13. The boundary-layer calculation can be restarted at any station by inputting the values of the variables at that station as listed in the output. The calculated list of $\delta^* + r_w$ and u_e/u_{e_o} will be written on Logical Unit 10 (data file 4) when the calculation terminates.

Another method is also available for calculating the boundary layer alone. The boundary-layer step of a viscid-inviscid iteration can be executed separately. The appropriate values on the fourth card would be:

LPROG	=	0
NRSTRT	=	0 or 1
NPRINT	=	0 or 1
N1MAX	=	100
N1	=	1
N2	=	21
N3	=	21
IBL	=	0
MIT2		(not needed)

This option requires input of all quantities as though the iterative sequence were to be completed. With the values just described, only the boundary layer will be calculated and then the run will be terminated. If it is desired to continue the iteration, simply make N1MAX equal the desired convergence percentage, make N2 and N3 less than 21, and put in an appropriate value for MIT2. The free-stream velocity distribution must be provided on Logical Unit 12 for this case. All other optional inputs are the user's choice.

7.2 INVISCID-FLOW OPTION

To use only the inviscid-flow program, put in the three card description, then put in LPROG = -1 on the fourth card (item number 2 in Table II). Of the remaining values on that card, only NPRINT is required. The value of NPRINT is the user's choice. After the first four cards only the data for items 3 to 7 as described in Table II and section 6 are required for this option.

7.3 VISCID-INVISCID ITERATION OPTION

To use both the boundary-layer and the inviscid-flow programs iteratively, put in LPROG = 0 and all other quantities as appropriate. Such iterations can be started with only the body shape and free-stream flow quantities known and may be restarted to continue a prematurely terminated iteration. Several options are available to the user for restarting an unfinished iteration. See section 10.2 for an example of restarting. The simplest option is to put in NRSTRT = 1 as the second value on the fourth input data card and to provide the required input data files on Logical Units 11, 12, 13, 14, and 15 (see fig. 3 and Table I). The required values of the remaining variables on card number 4 are printed periodically in the output. See section 8.1, step 20 of the output list. The particular set of values needed for restart is the last set printed before termination. The only other data required for restarting are the three-card description of the case. The calculation then proceeds from where the previous iteration stopped. Another method of restarting would be to omit the restart file and put in NRSTRT = 0. The user can then vary any of the other input quantities, using the data files or punched cards as desired. Note that the calculation terminates when N2 or N3 reach a value of 21. The value of N1 increases continuously throughout the calculation while the value of N2 is reset to 1 each time the θ_s cycle is converged. If the x_s iteration cycle has not converged when N3 reaches the value of 21, that value must be decreased in order to continue.

7.4 BOUNDARY-LAYER INITIAL CONDITIONS

Initial values of boundary-layer quantities can be obtained in several ways. The user can obtain values of the skin-friction coefficient, C_f, and either the boundary-layer thickness, δ, or the displacement thickness, δ^*. These are shown on item 16 in Table II. The appropriate values LSHAPE = 0 and LIC = 1 or 2 are then punched on the card corresponding to item 11. For the case when no other source of this information is available, formulas have been included in the program based on the Blasius solution for laminar boundary layers and based on one-seventh power law velocity profiles for turbulent flows. These formulas are only available if u_e is being specified (IOPT = 1). The basic formulas calculate C_f and δ in the transform plane (incompressible, two-dimensional). The formulas are as follows:

Laminar Flow

$$C_{f_i} = \frac{0.664}{\sqrt{\frac{U_e}{\nu_{e_o}} x}} \tag{50}$$

$$\delta_i = \frac{5x}{\sqrt{\frac{U_e}{\nu_{e_o}} x}} \tag{51}$$

Turbulent Flow

$$C_{f_i} = 0.0592 \left(\frac{U_e}{\nu_{e_o}} x\right)^{-0.2} \tag{52}$$

$$\delta_i = 0.37\, x \left(\frac{U_e}{\nu_{e_o}} x\right)^{-0.2} \tag{53}$$

These formulas provide initial values for boundary layers on flat plates. They are chosen by inputting LSHAPE = 1. For other geometries, the value of the x coordinate is transformed. Thus, LSHAPE = 2 chooses the values for a circular cylinder, where

$$x = x_a \left(\frac{r_w}{L}\right)^2 \tag{54}$$

where x_a is the axial coordinate and LSHAPE = 3 chooses the values for a cone, where

$$x = \frac{1}{3} x_a \left(\frac{r_w}{L}\right)^2 \tag{55}$$

These formulas have been found to be quite adequate for calculating flows over long bodies. Small initial errors in the calculated boundary layer become negligible in a few boundary-layer thicknesses.

8.0 PROGRAM OUTPUT

8.1 STANDARD OUTPUT

Several options are available for output from the programs. The parameter NPRINT on item number 2 in Table II chooses either all the available output (NPRINT = 1) or only that essential for monitoring the progress of an iterative calculation. The parameter DXP on item 15 controls the printing of boundary-layer velocity profiles. For iterative calculations, the output from the inviscid-flow program is controlled by NPRINT only on the first iteration (N1 = 1). For subsequent iterations, only the short form output is printed as if NPRINT = 0.

The complete program output is presented in the following list. Steps 1-10 are always printed for the first iteration.

Of the remaining steps, those denoted by an asterisk (*) are those printed when NPRINT = 0.

1. Three-line title or description.
2. List of all values of integers on first data card.
3. List of Body Geometry input.
4. List of other input values for inviscid flow.
5. List of input values for boundary-layer calculation.
6. List of Body Shape data for boundary layer.
7. List of other boundary-layer input quantities.
8. List of Variables used in inviscid-flow calculation. This includes the body geometry and other parameters.
9. Computed geometric parameters in normal direction for inviscid flow.
   - J - Normal grid index.
   - AN - Normal coordinate.
   - G - Stretching function derivative (refs.1 and 8).
   - GH - Stretching function derivative at half intervals.
10. Computed geometric parameters in tangential direction.
    - I - Tangential grid index.
    - S - Arc length along reference surface
    - X - Axial coordinate.
    - Y - Radial coordinate.
    - THET - Angle of reference coordinate surface, θ. For closed bodies, θ is the same as the body angle, θ_B. For open bodies, $\theta = \theta_B$ on the forebody and $\theta = 0$ on the afterbody.
    - THETB - Body angle, θ_B.
    - AK - Surface curvature on closed bodies. For open bodies AK is the surface curvature on the forebody and AK = $-(d^2 r_w/dx^2)$ on the afterbody.

10. (conc.) F - Derivative of the tangential stretch function (refs. 1 and 8).

*11. Inviscid relaxation iteration history.

IT - Iteration number.

DPMAX - Maximum ϕ correction, $\max_{ij}\left|\phi_{ij}^{IT} - \phi_{ij}^{IT-1}\right|$

ID,JD - I and J location of DPMAX.

RMAX - Maximum residual, $\max_{ij}\left|R_{ij}\right|$, where R_{ij} is the right-hand side of the difference equation.

IR,JR - I and J location of RMAX.

ISUB,ISUP - Indicates if maximum residual occurred at a subsonic or supersonic point.

RAVG - Average value of the residual.

RF1 - Relaxation factor for subsonic points.

QF3 - Relaxation factor for supersonic points.

NS - Number of supersonic points.

SEC/CY - Time for iteration cycle.

12. List of solution of perturbation potential.

*13. Tabulated values of surface pressure coefficient, C_p, Mach number, and axial velocity on the body along with a rough plot of C_p along the body. This plot is distorted in the axial direction because it is for equal spacing in the computational space. The asterisks show the level of sonic C_p.

*14. Drag coefficient by trapezoidal and Simpson integration of the C_p's on the real body. The displacement surface is removed for calculation of the drag.

(NOTE: If the two values differ greatly, it is probably due either to the computational mesh for the inviscid flow being too coarse or the inviscid relaxation being not sufficiently converged.)

15. Mach number chart of the flow field in the computational plane. Numbers printed are the Mach number multiplied by 100. The I values are from top to bottom and the J values are from left to right.

16. Coordinates x and y of the sonic line.

17. Boundary-layer reference velocity, u_{e_o}, and unit Reynolds number, R_{e_o}/L.

*18. List of boundary-layer quantities with profiles at intervals governed by DXP.

AX	-	Axial distance from the nose, x.
UTAU	-	Friction velocity, u_τ.
DELTA	-	Boundary-layer thickness, δ.
DELST	-	Displacement thickness, δ^*.
THETA	-	Momentum thickness, θ.
CF	-	Skin-friction coefficient, C_f.
UE/UZ	-	Free-stream velocity ratio, u_e/u_{e_o}.
CP	-	Surface pressure coefficient, C_p.
DELST+R	-	Augmented body radius, $\delta^* + r_w$.
DX	-	Integration step size.
HTR	-	Transformed shape factor, δ_i^*/θ_i.

*19. Quantities showing status of inner iteration.

XMAX	-	Location of maximum change in boundary layer δ^* from previous iteration.
DPMAX	-	Maximum change in δ^*.
DSMAX	-	Value of δ^* at XMAX.

*20. Quantities needed for restart. These are the values required on input card number 4. Note, however, that the restart procedure requires the particular set of these values which is the last to be printed before termination if the restart file (data file 5) is to be used (see section 10.2).

21. Rough plot and list of u_{e_V} and u_{e_I}. This is printed at the end of the inner iteration cycle whenever a new comparison is being made between the viscous and inviscid velocities.

8.2 SPECIAL OUTPUT MESSAGES

Several special messages are contained in the output to call attention to specific conditions that may occur. The messages are listed in this section with instructions about what to do when they are encountered.

(1) ---------DIVERGENCE.RMAX EXCEEDS RCHEK.
GO DIRECTLY TO JAIL. DO NOT PASS GO.
DO NOT COLLECT $200.------

This message is printed by the inviscid-flow program if the relaxation procedure diverges. Check all input to verify that it is correct. If no obvious errors appear, the difficulty is probably either in the choice of parameters for the computational mesh, or the smoothness of the data defining the body shape.

(2) RF1 DECREASED TO ____ BECAUSE 10-CYCLE AVG FOR RMAX INCREASED.

This message refers to the subsonic relaxation factor in the inviscid-flow program. The initial value is 1.4. The value is automatically reduced by 10 percent if: (1) the maximum residual, averaged over 10 cycles, is greater than that for the previous 10 cycles and (2) the last maximum residual occurred at a subsonic point.

(3) QF3 INCREASED TO ____ BECAUSE 10-CYCLE AVERAGE OF RMAX INCREASED.

This message refers to the supersonic damping factor in the inviscid-flow program. The initial value is 0.1. The value is automatically increased if: (1) the maximum correction, averaged over 10 cycles, is greater than that for the previous 10 cycles, and (2) the last maximum residual is at a supersonic point.

(4) INPUT FROM TAPE13 HAS INCOMPATIBLE DIMENSIONS

This message is printed if the dimensions of the ϕ_{ij} solution read from Logical Unit 13 (data file 2 in figure 3) are not the same as the values of IMAX and JMAX put on item number 6 in Table II.

(5) ****ITERATION FOR BOUNDARY LAYER/INVISCID FLOW EQUILIBRIUM CONVERGED

This message is printed whenever the maximum change in δ^* between iterations is less than the specified percent.

(6) METHOD FOR CALCULATING UTAU IN DERIV DOES NOT CONVERGE

This message refers to the iteration used to solve equation (43) for U_τ when δ^* is prescribed in the boundary-layer calculation. The only known cause of the iteration failing to converge is an error in the input data.

(7) DELTAI HAS BECOME NEGATIVE
STOP INTEGRATION, PRINT PROFILE AT PREVIOUS STEP

This message refers to the transformed boundary-layer thickness, δ_i. The error condition may occur due to the initial integration step size DXZ being too large. Another possible cause might be a too sudden change in the body shape, or in the prescribed u_e or δ^* distribution.

(8) DELTA HAS BECOME NEGATIVE
STOP INTEGRATION, PRINT VALUES AT PREVIOUS STEP

This message is not expected to occur in the finished program. If it does, check the input data carefully.

(9) INTEGRATION INTERVAL HAS BECOME TOO SMALL.

This message usually occurs when the singularity at $U_\tau = 0$ is approached in a positive pressure gradient with u_e prescribed. It may also occur under certain other conditions.

(10) METHOD FOR CALCULATING INITIAL VALUE OF DELI DOES NOT CONVERGE

When initial values of C_f, δ, or δ^* are known, the calculation must solve an integral equation for the initial value of the transformed thickness, δ_i. This is done by iteration in a similar manner as for u_τ described in message (6). If the iteration does not converge, it is usually due to errors in the input quantities.

(11) INTERMEDIATE RESULTS OF THETA ITERATION

This message is printed at the end of each step of the θ_s cycle. It is followed by the current value of the θ_s increment, DTHET and the value of the squared deviation, DIFFS.

(12) FINAL RESULTS OF THETA ITERATION

This message is printed whenever the θ_s cycle discussed in section 4.3 has converged. The message is followed by a list of the values of XSEP, DTHET, and the squared error for the best solution of that cycle.

(13) FINAL RESULTS OF XSEP ITERATION

This message is printed whenever the least squared error has been found for the x_s cycle discussed in section 4.3. When this condition occurs, the values of θ_s and x_s are set

to those corresponding to the best solution and the calculation reenters the inner cycle to perform a final iteration sequence. The final output of the inviscid-flow and boundary-layer solutions then correspond to the final converged solution.

(14) **********SOLUTION CONVERGED TO LEAST SQUARED ERROR TOLERANCE

This message is printed whenever the squared error is less than 0.0005 at any stage of the iteration. The inviscid and viscous solutions immediately preceding this message are then the best solutions of the calculation procedure.

(15) SKIN FRICTION HAS BECOME NEGATIVE IN AN INCORRECT MANNER. CHECK ALL INPUT CAREFULLY

This message will be printed if the skin-friction coefficient changes sign suddenly. This has been known to occur on rare occasions when the friction was approaching zero and the singularity did not cause the integration step size to decrease sufficiently to stop the calculation before a negative value of C_f was calculated. In such a case the calculation may be all right. The condition has also occurred at other times when an input error caused a discontinuity in the prescribed u_e.

9.0 PROGRAM OPERATING PROCEDURE

In this section, the construction of card decks for operation of the computer programs is described. First, a general description of the operations required is given. Then the specific Job Control cards needed for operation on an IBM 370 computer are listed. The same card decks should be applicable at any 370 installation with minor modifications.

9.1 GENERAL JOB CONTROL SEQUENCE

The following list is the general Job Control procedure that would be required to run the programs for a complete viscid-inviscid interaction calculation. The reader is referred to figure 3 and Table I.

1. Create partitioned data sets for restart files (files 1-5 in figure 3).
2. Define units 2, 3, 8, 9, and 10. These unit numbers are needed for output.
3. Define units 11, 12, 13, 14, and 15 if NRSTRT = 1 in the input data. These unit numbers correspond to the input files. They contain data created in a previous run.

For starting an initial calculation, the partitioned data sets would be created in a separate operation. Then, since no data would be on file, only units 2, 3, 8, 9, and 10 need to be defined. For restarting an iterative calculation, all data files would exist, so units 11 to 15 must also be defined.

To execute the boundary-layer program alone, unit 10 must be defined in order to output the $\delta^* + r_w$ and u_e/u_{e_o} list. Unit 12 must be defined when LVAR1 = 2, and unit 15 must be defined when LDSTAR = 1.

To execute the inviscid program alone, units 2 and 8 must be defined. Unit 13 is also required when LREADP = 1, and unit 14 is required when IXY = 0.

9.2 JOB CONTROL EXAMPLES

In this section, specific examples of Job Control cards used for the operations discussed previously are presented. In the examples, the computer program is referred to as "ITER" with the source code names "SITER" and the load module or binary

version named "BITER". The account ID used in the examples is WYL.XM.K01. Logical units 5 and 6 are the standard input/output file numbers. It is not necessary to specifically define these unit numbers in the JCL deck.

9.2.1 Creating Partitioned Data Sets

Partitioned data sets for use as input/output disk files must be created before the normal program operation can proceed. The following procedure is suggested:

Use IBM Utility Program IEFBR14.

Use default values for DCB (DSORG=PO,RECFM=VS).

On 3330 disk, use SPACE in tracks as follows (refer to figure 3 and Table I for explanation of file numbers):

VELBOD	(File 3)	SPACE = (TRK,(2,1,10))
RESTRT	(File 5)	SPACE = (TRK,(10,2,10))
PHI	(File 2)	SPACE = (TRK,(20,4,10))
XOFILE	(File 1)	SPACE = (TRK,(4,1,10))
DSFILE	(File 4)	SPACE = (TRK,(6,1,10))

Example of creating a partitioned data set called VELBOD:

```
//EXEC PGM=IEFBR14
//A DD DSN=WYL.XM.K01.VELBOD,VOL=volume,
//      UNIT=3330,DISP=(,CATLG),
//      SPACE=(TRK,(2,1,10))
```

9.2.2 Starting an Iteration Sequence

To start an iteration sequence, unit numbers 2, 3, 8, 9, and 10 must be defined. The specific sequence of cards used to perform the calculations presented in section 10.1 is as follows:

```
// EXEC FORTGO,PROG=ITER,VOL=volume
//        LIB='WYL.XM.K01.BITER'
//GO.FT02F001 DD DSN=WYL.XM.K01.VELBOD(RUN1),
//        DISP=OLD
//GO.FT03F001 DD DSN=WYL.XM.K01.RESTRT(RUN1),
//        DISP=OLD
//GO.FT08F001 DD DSN=WYL.XM.K01.PHI(RUN1),
//        DISP=OLD
//GO.FT09F001 DD DSN=WYL.XM.K01.XOFILE(RUN1),
//        DISP=OLD
//GO.FT10F001 DD DSN=WYL.XM.K01.DSFILE(RUN1),
//        DISP=OLD
//GO.SYSIN DD *
        {  Input data cards
/*
```

9.2.3 Restarting an Iteration Sequence

The specific cards used to perform a restart of the calculation started in the previous section are:

```
// EXEC FORTGO,PROG=ITER,VOL=volume,
//        LIB='WYL.XM.K01.BITER'
//GO.FT02F001 DD DSN=WYL.XM.K01.VELBOD(RUN2),
//        DISP=OLD
//GO.FT03F001 DD DSN=WYL.XM.K01.RESTRT(RUN2),
//        DISP=OLD
//GO.FT08F001 DD DSN=WYL.XM.K01.PHI(RUN2),
//        DISP=OLD
//GO.FT09F001 DD DSN=WYL.XM.K01.XOFILE(RUN2),
//        DISP=OLD
//GO.FT10F001 DD DSN=WYL.XM.K01.DSFILE(RUN2),
//        DISP=OLD
```

```
//GO.FT11F001 DD DSN=WYL.XM.K01.RESTRT(RUN1),
//        DISP=OLD,LABEL=(,,,IN)
//GO.FT12F001 DD DSN=WYL.XM.K01.VELBOD(RUN1),
//        DISP=OLD,LABEL=(,,,IN)
//GO.FT13F001 DD DSN=WYL.XM.K01.PHI(RUN1),
//        DISP=OLD,LABEL=(,,,IN)
//GO.FT14F001 DD DSN=WYL.XM.K01.XOFILE(RUN1),
//        DISP=OLD,LABEL=(,,,IN)
//GO.FT15F001 DD DSN=WYL.XM.K01.DSFILE(RUN1),
//        DISP=OLD,LABEL=(,,,IN)
//GO.SYSIN DD *
        { Input data cards
/*
```

These cards were used with the example discussed in section 10.2.

9.2.4 Executing the Boundary-Layer Program Alone

The specific cards used to perform the calculations discussed in section 10.3 are listed in this section. In the example shown here, all input is assumed to be from cards, but the output list of $\delta^* + r_w$ and u_e/u_{e_o} is to be saved on unit 10. Unit 12 would be required for input if LVAR1 = 2, and unit 15 would be required if LDSTAR = 1. The cards used in the example in section 10.3 are:

```
// EXEC FORTGO,PROG=ITER,VOL=volume
//        LIB='WYL.XM.K01.BITER'
//GO.FT10F001 DD DSN=WYL.XM.K01.DSFILE(RUN1),
//        DISP=OLD
//GO.SYSIN DD *
        { Input data cards
/*
```

9.2.5 Executing the Inviscid Program Alone

The cards used to perform the calculations discussed in section 10.4 are listed in this section. In this example, the velocity potential, ϕ, is input from unit 13, and the new solution for ϕ is output on unit 8. The calculated velocity on the body is output on unit 2. Input from unit 13 corresponds to LREADP = 1 in the card input data. In addition, unit 14 would be required for input of the body shape if IXY = 0 in the card input data. The specific cards used in the example are:

```
// EXEC FORTGO,PROG=ITER,VOL=volume,
//       LIB='WYL.XM.K01.BITER'
//GO.FT02F001 DD DSN=WYL.XM.K01.VELBOD(RUN2),
//       DISP=OLD
//GO.FT08F001 DD DSN=WYL.XM.K01.PHI(RUN2),
//       DISP=OLD
//GO.FT13F001 DD DSN=WYL.XM.K01.PHI(RUN1),
//       DISP=OLD,LABEL=(,,,IN)
//GO.SYSIN DD *
      {  Input data cards
/*
```

10.0 NUMERICAL EXAMPLES

In this section, several example calculations are presented to aid in program checkout. An example is presented of a complete viscid-inviscid interaction, starting from the initial input and restarting after premature termination. An example is also presented of the use of the boundary-layer program alone for a two-dimensional geometry. That example also demonstrates the two options for boundary conditions, having u_e specified in the

beginning of the calculation, and δ^* specified in the second part. Input data for another sample case are also presented to demonstrate the use of the program to calculate the inviscid flow alone.

10.1 AXISYMMETRIC INTERACTION

A list of the punched card input data for a sample calculation on the boattailed body shown in figure 4 is presented in figure 5. The case being calculated is for a free-stream Mach number of 0.9. The body corresponds to the ogive-cylinder body with a circular-arc-conic boattail described in reference 11. The JCL card deck for this case has been presented in section 9.2.2. The running time for the complete calculation is about 10 minutes on the IBM 370/165.

Selected output for the sample case is shown in figure 6. A total of 27 iterations were calculated. The best solution was determined to be that corresponding to the values of x_s and θ_s used for iteration 20. Those values are used in iteration 27 to produce a final list of the solution so that it is not necessary to search through the output for the best solution. However, some caution is required in interpreting the final output. The agreement between the u_{e_V} and the u_{e_I} for the final inviscid and viscous solutions is somewhat dependent upon the accuracy of the previous calculations as determined by the input quantities N1MAX and DFACT. For the calculations shown in figure 6, N1MAX had a value of 7 and DFACT had a value of 0.5. A smaller value of N1MAX and a larger value of DFACT should improve the final agreement.

The complete list of output for this case, with NPRINT = 0, consisted of a total of 6661 lines. Output steps 1-7 as listed in section 8.1 have been omitted from this presentation since they simply verify the input data. The output pages shown are those corresponding to steps 8-21 of the set described in

section 8.1 for NPRINT = 0 on the first iteration and then a few samples of the rough plots of u_{eV} and u_{eI} at intermediate steps, including that at iteration 20 (fig. 6(j)). Finally, figure 6 concludes with the inviscid solution and boundary-layer solution corresponding to the final result.

10.2 EXAMPLE OF RESTARTING AN INTERACTION CALCULATION

The punched card input data for restarting the interaction calculation of section 10.1 after premature termination at the twelfth iteration (eleven complete iterations) is presented in figure 7. See figure 6(i) for the printed output of these quantities. The JCL card deck for this calculation was presented in section 9.2.3. Note that the iterative calculations cannot be restarted at any arbitrary iteration using the restart file, unit 11. That file and the other output files contain only the data that were output just prior to the termination.

10.3 TWO-DIMENSIONAL BOUNDARY LAYER

A list of the punched card input data for a sample calculation on the two-dimensional configuration shown in figure 8 is presented in figure 9. Note that two sets of input are presented for this case, giving an example of the options of prescribed u_e and prescribed δ^*. The data for u_e and δ^* were obtained from the experimental results of reference 12 which indicate separation occurring in an adverse pressure gradient region downstream of a shock wave. The output for the complete boundary-layer calculation are presented in figure 10. No external data files were used for input for this case. The JCL card deck for this case was presented in section 9.2.4.

10.4 AXISYMMETRIC INVISCID FLOW

The punched card input data for a sample calculation of the inviscid flow alone are presented in figure 11. These data correspond to the first inviscid-flow step of the iteration calculation described in section 10.1. The output for this case is the same as that shown in figure 6(a) through (e).

REFERENCES

1. Keller, J. D. and South, J. C., Jr.: RAXBOD: A FORTRAN Program for Inviscid Transonic Flow Over Axisymmetric Bodies. NASA TM X-72831, Feb. 1976.

2. Kuhn, G. D.: Calculation of Compressible, Nonadiabatic Boundary Layers in Laminar, Transitional and Turbulent Flow by the Method of Integral Relations. NASA CR-1797, Nov. 1971.

3. Probstein, R. F. and Elliott, D.: The Transverse Curvature Effect in Compressible Axially Symmetric Laminar Boundary-Layer Flow. J. Aero. Sci., vol. 23, 1956, p. 208.

4. Stewartson, K.: Correlated Incompressible and Compressible Boundary Layers. Proc. of the Royal Soc., A, vol. 200, 1949, pp. 85-100.

5. Kuhn, G. D. and Nielsen, J. N.: An Analytical Method for Calculating Turbulent Separated Flow Due to Adverse Pressure Gradients. Project SQUID Tech. Rept. NEAR-1-PU, Oct. 1971.

6. Coles, D.: The Law of the Wake in the Turbulent Boundary Layer. J. Fluid Mech., vol. 1, pt. 2, 1956, pp. 191-226.

7. Kuhn G. D. and Nielsen, J. N.: Prediction of Turbulent Separated Boundary Layers. AIAA Journal, vol. 12, no. 7, July 1974, pp. 881-882.

8. South, J. C., Jr. and Jameson, A.: Relaxation Solutions for Inviscid Axisymmetric Transonic Flow Over Blunt or Pointed Bodies. AIAA Computational Fluid Dynamics Conference Proceedings, Palm Springs, CA, July 1973, pp. 8-17.

9. Presz, W. M., Jr.: Turbulent Boundary Layer Separation of Axisymmetric Afterbodies. Ph.D. Thesis, University of Connecticut, 1974.

10. Reubush, D. E. and Putnam, L. E.: An Experimental and Analytical Investigation of the Effect on Isolated Boattail Drag of Varying Reynolds Number up to 130×10^6. NASA TN D-8210, May 1976.

11. Blaha, B. J., Chamberlin, R., and Bober, L. J.: Boundary Layer Thickness Effect on Boattail Drag. AIAA Paper No. 76-676 presented at Twelfth Propulsion Conference, Palo Alto, CA, July 26-29, 1976.

REFERENCES (CONCLUDED)

12. Alber, I. E., Bacon, J. W., Masson, B. S., and Collins, D. J.: An Experimental Investigation of Turbulent Transonic Viscous-Inviscid Interactions. AIAA Journal, vol. 11, no. 5, May 1973, pp. 620-627.

TABLE I. RELATION BETWEEN EXTERNAL DATA SETS AND INPUT/OUTPUT LOGICAL UNIT NUMBERS

Data File (fig. 3)	Logical Unit	
	Input	Output
1	14	9
2	13	8
3	12	2
4	15	10
5	11	3

TABLE II. INPUT DATA CARDS

CARD ORDER	VARIABLES	FORMAT
1	TITLE (three cards)	20A4
2	LPROG,NRSTRT,NPRINT,N1MAX,N1,N2,N3,IBL,MIT2	16I5
3	GAMMA,AMINF	8F10.0
	If LPROG=1, skip to item no. 11. If LPROG=0, put in all cards as required. If LPROG=0 and NRSTRT>0, stop. No further cards are needed.	
4	IXY	16I5
	If IXY=0, skip next card.	
5	XO,YO	2F10.0
6	IMAX,JMAX,MIT,MHALF,KLOSE,NPLOT,LREADP	16I5
7	DETAO,XIXM,XM,XIM1,XBT	8F10.0
	If LPROG=-1, skip remaining cards.	
8	XZNEW,DTHET	8F10.0
9	LSEP	L5
	If LSEP=FALSE, skip next card.	
10	XSEP	8F10.0
11	IOPT,K,LVAR1,LSHAPE,LIC,LDSTAR,IUNIT,LSHPBL	16I5
	If LPROG≠1 or if LPROG=1 and both IOPT=1 LVAR1=2, skip items 12 and 13.	
12	NVAR	16I5

TABLE II. CONCLUDED

CARD ORDER	VARIABLES	FORMAT
13	XVAR,VAR	8F10.0
14	EL,PT,TT,TWONTT,VISC,RGAS,SCON,DFACT	8F10.0
15	XZ,RLEN,XT,DXZ,DXP,DXOUT,HLIM	8F10.0
	If LSHAPE≠0, skip next card. If LIC=1, input CFC1 and DELTA1. If LIC=2, input CFC1 and DELST1.	
16	CFC1,DELTA1 (or DELST1)	8F10.0
	If IOPT=1, skip next card.	
17	UE1,DUEDX	8F10.0
	If LSHPBL=0 and LPROG=0, skip items 18 and 19.	
18	NR	16I5
19	XRP,RL	2F10.0

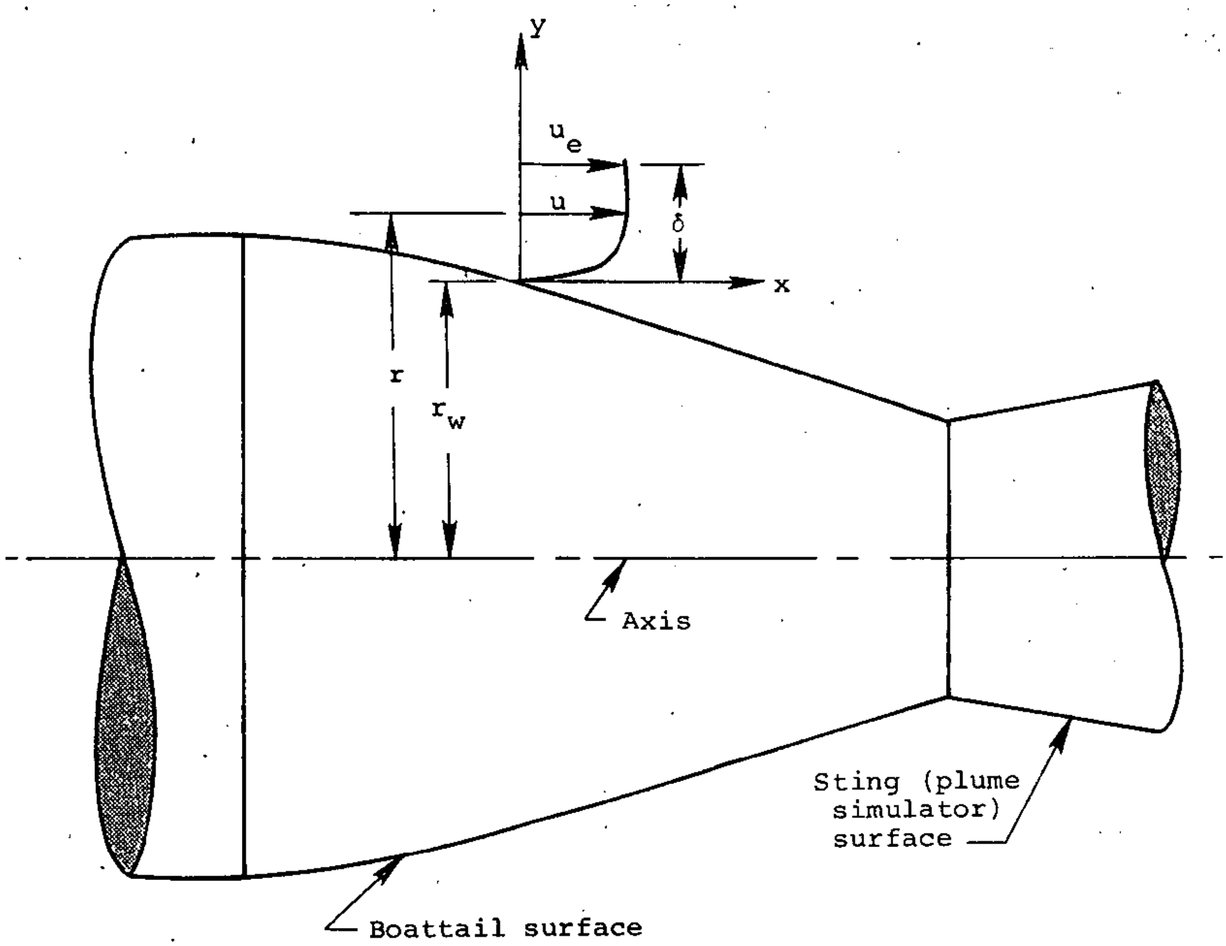

Figure 1. Boundary-layer coordinate system.

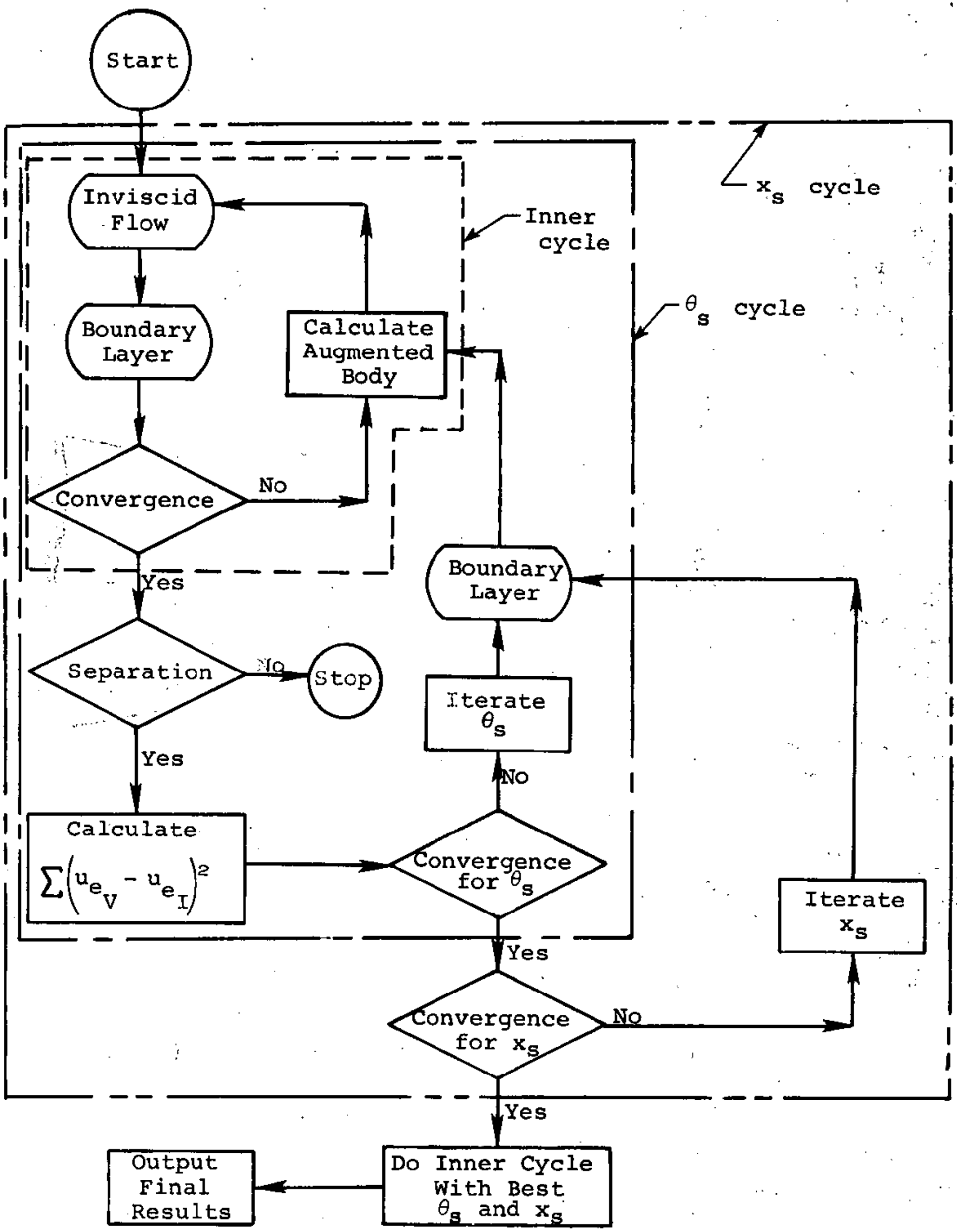

Figure 2. Schematic of iteration procedure.

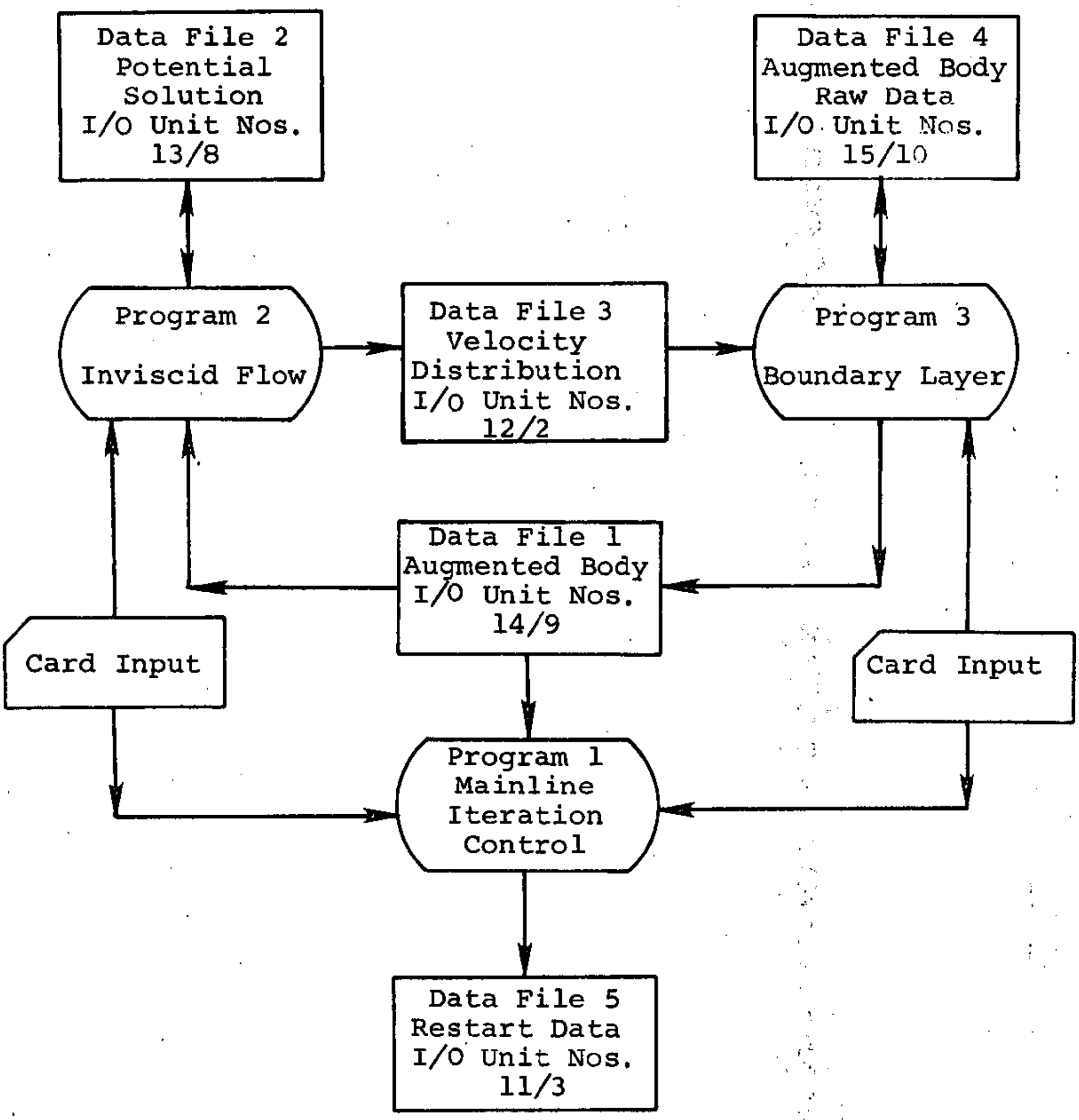

Figure 3. General relationship of programs and data files.

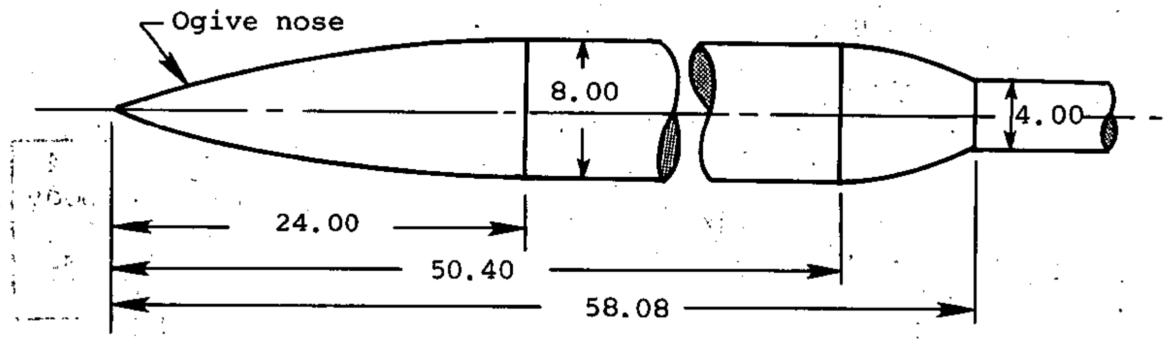

(a) Overall body geometry.

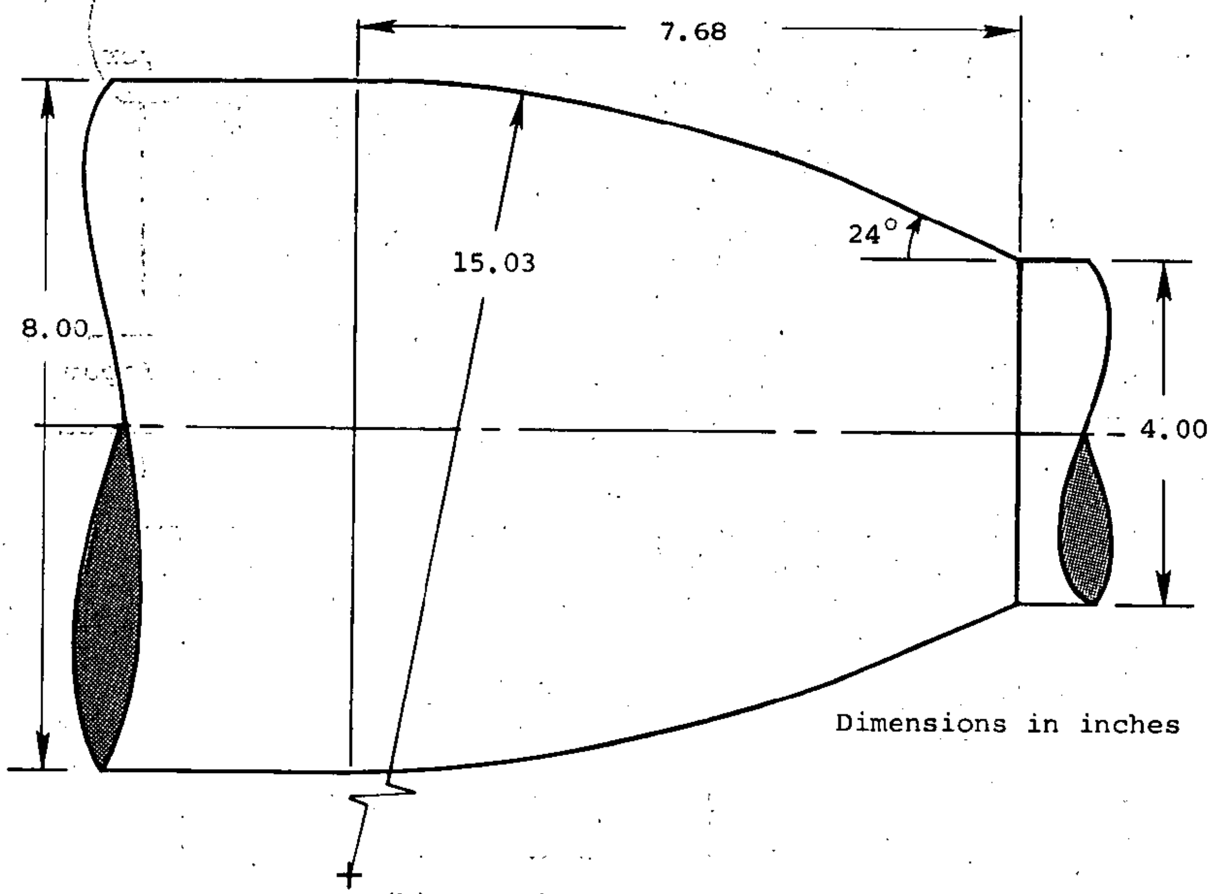

(b) Detailed boattail geometry.

Figure 4. Axisymmetric body for sample calculation.

```
BLAHA,CHAMBERLIN AND BOBER  6524  BOATTAIL-STING
TESTING COMPLETE ITERATION
TRANSONIC FLOW WITH WEAK SHOCK ON AFTERBODY
    0    0    0    7    1    1    1    1   10
    1.4       0.9
   53
    0.0       0.0
    0.25      0.085
    0.50      0.17
    0.75      0.255
    1.0       0.34
    1.5       0.49
    2.0       0.64
    4.0       1.2
    6.0       1.68
    8.0       2.13
   10.0       2.56
   12.0       2.92
   14.0       3.24
   16.0       3.5
   18.0       3.65
   20.0       3.80
   22.0       3.91
   24.0       4.0
   26.0       4.0
   30.0       4.0
   35.0       4.0
   40.0       4.0
   45.0       4.0
   50.0       4.0
   50.4       4.0
   50.5       3.9997
   50.7       3.997
   51.0       3.988
   51.25      3.9759
   51.5       3.9597
   51.75      3.9392
   52.0       3.9146
   52.5       3.8525
   53.0       3.7733
   53.5       3.6767
   54.0       3.5624
   54.5       3.4298
```

(a) First 43 cards.

Figure 5. Input data for interaction calculation on body of figure 4.

```
55.0       3.2786
55.5       3.1080
56.0       2.9175
56.5       2.7061
57.0       2.4835
57.5       2.2609
58.08      2.0
58.5       2.0
59.0       2.0
59.5       2.0
60.0       2.0
60.5       2.0
61.0       2.0
62.0       2.0
63.0       2.0
64.0       2.0
51   31   10    0     0    0     0
 0.25      0.84       58.08      80.0       58.08
52.0       0.0
 F
 1    1    2    3     1    0     2    0
 1.0       16.81     590.0       0.97
 2.0       64.0        6.0       0.001      0.0       0.5
```

(b) Remaining 23 cards.

Figure 5. Concluded.

```
VALUES OF VARIABLES USED IN INVISCID FLOW CALCULATION

IMAX JMAX  MIT MHALF KLOSE NPLOT READP
  51   31   20     0     0     0     0

 RF10        COVERG      QF3
0.140E+01 0.100E+01 0.100E+00

 DSDXIO      DNDZO       XIXM        XM          DSDXIM
0.100E+02 0.574E+01 0.840E+00 0.581E+02 0.191E+02

 GAM         AMINF
0.140E+01 0.900E+00

       KSTAR  PSTAR       CPSTAR        CPO

          46  0.8935E+00 -0.1879E+00  0.1219E+01

               RMSQ        AMSQ        GM1         GM102       GOGM1       GMSQ        ADSQ        TOGMSQ

              0.1600E+02  0.8100E+00  0.4000E+00  0.2000E+00  0.3500E+01  0.1620E+00  0.1435E+01  0.1764E+01

               DXIO        DZ          DXISQ       DXIDZ       DZSQ        DZ2         DXI2

              0.2000E-01  0.3333E-01  0.2500E+04  0.7500E+03  0.9000E+03  0.1500E+02  0.2500E+02
```

(a) List of variables used in inviscid-flow calculation.

Figure 6. Selected output for calculation of viscid-inviscid interaction on boattailed body.

------ NORMAL COORD. STRETCH FOR ALF= 1.300 ------

J	AN	G	GH
1	-0.1361E 21	0.0	0.2704E-04
2	0.4619E 03	0.54[illegible]9E-04	0.1512E-03
3	0.1811E 03	0.2684E-03	0.4779E-03
4	0.1031E 03	0.6874E-03	0.1015E-02
5	0.6830E 02	0.1343E-02	0.18[illegible]2E-02
6	0.4914E 02	0.2261E-02	0.2864E-02
7	0.3722E 02	0.3467E-02	0.4225E-02
8	0.2919E 02	0.4982E-02	0.5906E-02
9	0.2347E 02	0.6829E-02	0.7928E-02
10	0.1922E 02	0.9029E-02	0.1031E-01
11	0.1597E 02	0.1160E-01	0.1308E-01
12	0.1340E 02	0.1456E-01	0.1625E-01
13	0.1134E 02	0.1794E-01	0.1985E-01
14	0.9649E 01	0.2175E-01	0.2388E-01
15	0.8247E 01	0.2602E-01	0.2839E-01
16	0.7068E 01	0.3076E-01	0.3337E-01
17	0.6066E 01	0.3599E-01	0.3887E-01
18	0.52[illegible]6E 01	0.4174E-01	0.4489E-01
19	0.4461E 01	0.4803E-01	0.5146E-01
20	0.3812E 01	0.5488E-01	0.5860E-01
21	0.3242E 01	0.6231E-01	0.6633E-01
22	0.2738E 01	0.7035E-01	0.7469E-01
23	0.2291E 01	0.7902E-01	0.8369E-01
24	0.1892E 01	0.8835E-01	0.9335E-01
25	0.1535E 01	0.9835E-01	0.1037E 00
26	0.1213E 01	0.1091E 00	0.1148E 00
27	0.9220E 00	0.1205E 00	0.1266E 00
28	0.6594E 00	0.1327E 00	0.1392E 00
29	0.4187E 00	0.1457E 00	0.1526E 00
30	0.2000E 00	0.1595E 00	0.1668E 00
31	0.3422E-06	0.1742E 00	0.1819E 00

(b) Computed geometric parameters in normal direction for inviscid flow.

Figure 6. Continued.

I	S	X	Y	THET	THETB	AK	F
1	0.0	0.0	0.0	0.9000E 02	0.9000E 02	0.1654E-02	0.1000E 00
2	0.2031E 00	0.1923E 00	0.6537E-01	0.1878E 02	0.1878E 02	0.2163E-02	0.9556E-01
3	0.4247E 00	0.4021E 00	0.1368E 00	0.1878E 02	0.1878E 02	0.5748E-02	0.8438E-01
4	0.6832E 00	0.6469E 00	0.2198E 00	0.1877E 02	0.1877E 02	0.2047E-01	0.7071E-01
5	0.9962E 00	0.9430E 00	0.3211E 00	0.1856E 02	0.1856E 02	0.1142E 00	0.5780E-01
6	0.1381E 01	0.1310E 01	0.4348E 00	0.1627E 02	0.1627E 02	0.3310E-01	0.4698E-01
7	0.1853E 01	0.1763E 01	0.5685E 00	0.1679E 02	0.1679E 02	0.1204E-01	0.3840E-01
8	0.2427E 01	0.2313E 01	0.7333E 00	0.1642E 02	0.1642E 02	0.1782E-01	0.3176E-01
9	0.3116E 01	0.2976E 01	0.9240E 00	0.1569E 02	0.1569E 02	0.1932E-01	0.2663E-01
10	0.3933E 01	0.3763E 01	0.1136E 01	0.1475E 02	0.1475E 02	0.2111E-01	0.2265E-01
11	0.4885E 01	0.4687E 01	0.1372E 01	0.1368E 02	0.1368E 02	0.1592E-01	0.1954E-01
12	0.5982E 01	0.5754E 01	0.1624E 01	0.1296E 02	0.1296E 02	0.7038E-02	0.1709E-01
13	0.7227E 01	0.6968E 01	0.1899E 01	0.1266E 02	0.1266E 02	0.2539E-02	0.1514E-01
14	0.8624E 01	0.8332E 01	0.2204E 01	0.1254E 02	0.1254E 02	0.3803E-02	0.1357E-01
15	0.1017E 02	0.9846E 01	0.2529E 01	0.1144E 02	0.1144E 02	0.2149E-01	0.1231E-01
16	0.1187E 02	0.1152E 02	0.2838E 01	0.9736E 01	0.9736E 01	0.1023E-01	0.1128E-01
17	0.1372E 02	0.1334E 02	0.3138E 01	0.8947E 01	0.8947E 01	0.8580E-02	0.1045E-01
18	0.1570E 02	0.1530E 02	0.3422E 01	0.7093E 01	0.7093E 01	0.3074E-01	0.9767E-02
19	0.1781E 02	0.1740E 02	0.3609E 01	0.3758E 01	0.3758E 01	0.1666E-02	0.9219E-02
20	0.2003E 02	0.1962E 02	0.3773E 01	0.4217E 01	0.4217E 01	0.1364E-01	0.8782E-02
21	0.2236E 02	0.2194E 02	0.3907E 01	0.2897E 01	0.2897E 01	0.6102E-02	0.8443E-02
22	0.2476E 02	0.2434E 02	0.4006E 01	0.1012E 01	0.1012E 01	0.2959E-01	0.8190E-02
23	0.2723E 02	0.2681E 02	0.3994E 01	0.0	-0.3637E 00	-0.7443E-02	0.8017E-02
24	0.2975E 02	0.2933E 02	0.3997E 01	0.0	0.2499E 00	0.3062E-03	0.7921E-02
25	0.3228E 02	0.3186E 02	0.4003E 01	0.0	0.3521E-02	0.1267E-02	0.7900E-02
26	0.3480E 02	0.3438E 02	0.4001E 01	0.0	-0.6941E-01	-0.2584E-03	0.7956E-02
27	0.3730E 02	0.3687E 02	0.3999E 01	0.0	-0.1268E-02	-0.3420E-03	0.8096E-02
28	0.3973E 02	0.3931E 02	0.4000E 01	0.0	0.2012E-01	0.3573E-04	0.8329E-02
29	0.4209E 02	0.4167E 02	0.4000E 01	0.0	0.4273E-02	0.1160E-03	0.8670E-02
30	0.4434E 02	0.4392E 02	0.4000E 01	0.0	-0.8391E-02	0.8056E-04	0.9141E-02
31	0.4646E 02	0.4604E 02	0.4000E 01	0.0	-0.1380E-01	-0.3185E-04	0.9773E-02
32	0.4843E 02	0.4800E 02	0.3999E 01	0.0	-0.1246E-04	-0.2128E-03	0.1061E-01
33	0.5022E 02	0.4980E 02	0.4000E 01	0.0	0.3039E-01	-0.3780E-03	0.1173E-01
34	0.5183E 02	0.5141E 02	0.3966E 01	0.0	-0.3842E 01	0.6865E-01	0.1322E-01
35	0.5325E 02	0.5282E 02	0.3803E 01	0.0	-0.9285E 01	0.6911E-01	0.1524E-01
36	0.5446E 02	0.5404E 02	0.3554E 01	0.0	-0.1400E 02	0.7384E-01	0.1802E-01
37	0.5547E 02	0.5505E 02	0.3264E 01	0.0	-0.1801E 02	0.7843E-01	0.2193E-01
38	0.5628E 02	0.5586E 02	0.2972E 01	0.0	-0.2132E 02	0.8382E-01	0.2751E-01
39	0.5693E 02	0.5651E 02	0.2703E 01	0.0	-0.2393E 02	0.7670E-01	0.3542E-01
40	0.5743E 02	0.5700E 02	0.2482E 01	0.0	-0.2320E 02	-0.1312E 00	0.4587E-01
41	0.5782E 02	0.5739E 02	0.2313E 01	0.0	-0.2512E 02	0.3377E 00	0.5662E-01
42	0.5815E 02	0.5773E 02	0.2138E 01	0.0	-0.2772E 02	-0.3410E 00	0.6055E-01
43	0.5850E 02	0.5808E 02	0.2000E 01	0.0	-0.1089E 02	-0.1565E 01	0.5226E-01
44	0.5894E 02	0.5852E 02	0.2001E 01	0.0	0.2811E 01	0.3684E 00	0.4001E-01
45	0.5952E 02	0.5910E 02	0.1999E 01	0.0	-0.3354E 00	-0.7695E-01	0.2940E-01
46	0.6034E 02	0.5992E 02	0.2000E 01	0.0	-0.8278E-01	-0.1566E-02	0.2042E-01
47	0.6156E 02	0.6114E 02	0.2000E 01	0.0	-0.3250E-02	-0.2913E-03	0.1307E-01
48	0.6360E 02	0.6318E 02	0.2000E 01	0.0	-0.1449E-03	-0.1984E-04	0.7350E-02
49	0.6769E 02	0.6726E 02	0.2000E 01	0.0	0.0	0.0	0.3267E-02
50	0.7993E 02	0.7951E 02	0.2000E 01	0.0	0.0	0.0	0.8167E-03
51	0.1000E 31	0.1000E 31	0.2000E 01	0.0	0.0	0.0	0.1000E-29

(c) Computed tangential geometric parameters.

Figure 6. Continued.

IT	DPMAX	ID	JD	RMAX	IR	JR	ISUB	ISUP	RAVG	RF1	QF3	NS	SEC/CYC
1	0.135E 00	42	31	0.109E 02	1	31	1	0	0.628E-01	1.400	0.100	0	0.200
2	0.998E-01	39	31	0.453E 01	42	31	1	0	0.489E-01	1.400	0.100	0	0.207
3	0.854E-01	38	31	0.349E 01	41	31	1	0	0.435E-01	1.400	0.100	0	0.197
4	0.760E-01	38	31	0.289E 01	41	31	1	0	0.397E-01	1.400	0.100	0	0.187
5	0.677E-01	38	31	0.318E 01	1	31	1	0	0.394E-01	1.400	0.100	0	0.193
6	0.607E-01	38	31	0.217E 01	39	31	1	0	0.366E-01	1.400	0.100	0	0.200
7	0.547E-01	38	31	0.194E 01	39	31	1	0	0.332E-01	1.400	0.100	0	0.197
8	0.498E-01	37	31	0.173E 01	39	31	1	0	0.312E-01	1.400	0.100	3	0.207
9	0.456E-01	37	31	0.154E 01	39	31	1	0	0.306E-01	1.400	0.100	5	0.207
10	0.417E-01	37	31	0.139E 01	38	31	1	0	0.299E-01	1.400	0.100	8	0.217
11	0.382E-01	37	31	0.126E 01	38	31	1	0	0.288E-01	1.400	0.100	9	0.200
12	0.350E-01	37	31	0.115E 01	38	31	1	0	0.276E-01	1.400	0.100	11	0.203
13	0.322E-01	37	31	0.105E 01	38	31	1	0	0.267E-01	1.400	0.100	12	0.213
14	0.297E-01	37	31	0.100E 01	42	31	1	0	0.260E-01	1.400	0.100	14	0.223
15	0.275E-01	36	31	0.100E 01	1	31	1	0	0.254E-01	1.400	0.100	15	0.207
16	0.256E-01	36	31	0.968E 00	1	31	1	0	0.247E-01	1.400	0.100	17	0.220
17	0.239E-01	36	31	0.915E 00	1	31	1	0	0.241E-01	1.400	0.100	17	0.200
18	0.224E-01	36	31	0.891E 00	1	31	1	0	0.235E-01	1.400	0.100	18	0.210
19	0.209E-01	36	31	0.891E 00	1	31	1	0	0.229E-01	1.400	0.100	19	0.197
20	0.196E-01	36	31	0.887E 00	1	31	1	0	0.224E-01	1.400	0.100	20	0.207

RMAX= 0.89E 00, COVR= 0.42E-03

(d) Iteration history for inviscid relaxation on plain body.

Figure 6. Continued.

PLOT CF CP AT EQUAL XI-INCREMENTS

I	XB	YB	FM	QS	CP
1	0.0	0.0	0.0	0.0	1.2192
2	0.192	0.065	0.854	0.955	0.0898
3	0.402	0.137	0.6[illegible]8	0.703	0.5595
4	0.647	0.220	0.666	0.764	0.4517
5	0.943	0.321	0.705	0.806	0.3768
6	1.310	0.435	0.730	0.831	0.3294
7	1.763	0.568	0.738	0.839	0.3144
8	2.313	0.733	0.763	0.865	0.2652
9	2.976	0.924	0.788	0.890	0.2163
10	3.763	1.138	0.811	0.913	0.1716
11	4.667	1.372	0.828	0.930	0.1389
12	5.754	1.624	0.837	0.939	0.1211
13	6.968	1.899	0.846	0.947	0.1047
14	8.332	2.204	0.866	0.968	0.0645
15	9.840	2.529	0.898	0.998	0.0045
16	11.517	2.838	0.913	1.012	-0.025[illegible]
17	13.327	3.138	0.929	1.028	-0.0554
18	15.290	3.422	0.967	1.063	-0.1270
19	17.399	3.609	0.950	1.047	-0.0952
20	19.618	3.773	0.927	1.025	-0.0508
21	21.939	3.907	0.950	1.047	-0.0945
22	24.344	4.006	0.948	1.046	-0.0919
23	26.814	3.994	0.919	1.018	-0.0365
24	29.325	3.997	0.904	1.004	-0.0071
25	31.856	4.003	0.906	1.006	-0.0114
26	34.381	4.001	0.902	1.002	-0.0044
27	36.875	3.999	0.901	1.001	-0.0013
28	39.313	4.000	0.901	1.001	-0.0025
29	41.669	4.000	0.902	1.002	-0.0042
30	43.918	4.000	0.904	1.003	-0.0068
31	46.037	4.000	0.907	1.007	-0.0131
32	48.004	3.999	0.916	1.016	-0.0313
33	49.801	4.000	0.979	1.074	-0.1496
34	51.411	3.960	1.085	1.167	-0.3413
35	52.824	3.803	1.114	1.178	-0.3901
36	54.036	3.554	1.025	1.083	-0.2337
37	55.046	3.264	0.912	0.962	-0.0225
38	55.864	2.972	0.832	0.873	0.1319
39	56.507	2.703	0.750	0.779	0.2900
40	57.004	2.482	0.697	0.733	0.3925
41	57.394	2.313	0.643	0.670	0.4950
42	57.730	2.138	0.514	0.531	0.7279
43	58.080	2.0[illegible]0	0.479	0.551	0.7850
44	58.517	2.001	0.606	0.700	0.5630
45	59.100	1.999	0.737	0.838	0.3159
46	59.917	2.000	0.800	0.902	0.1934
47	61.141	2.000	0.850	0.952	0.0954
48	63.182	2.000	0.882	0.982	0.0350
49	67.264	2.000	0.896	0.996	0.0081
50	79.509	2.000	0.900	1.000	0.0007
51	********	2.000	0.900	1.000	0.0

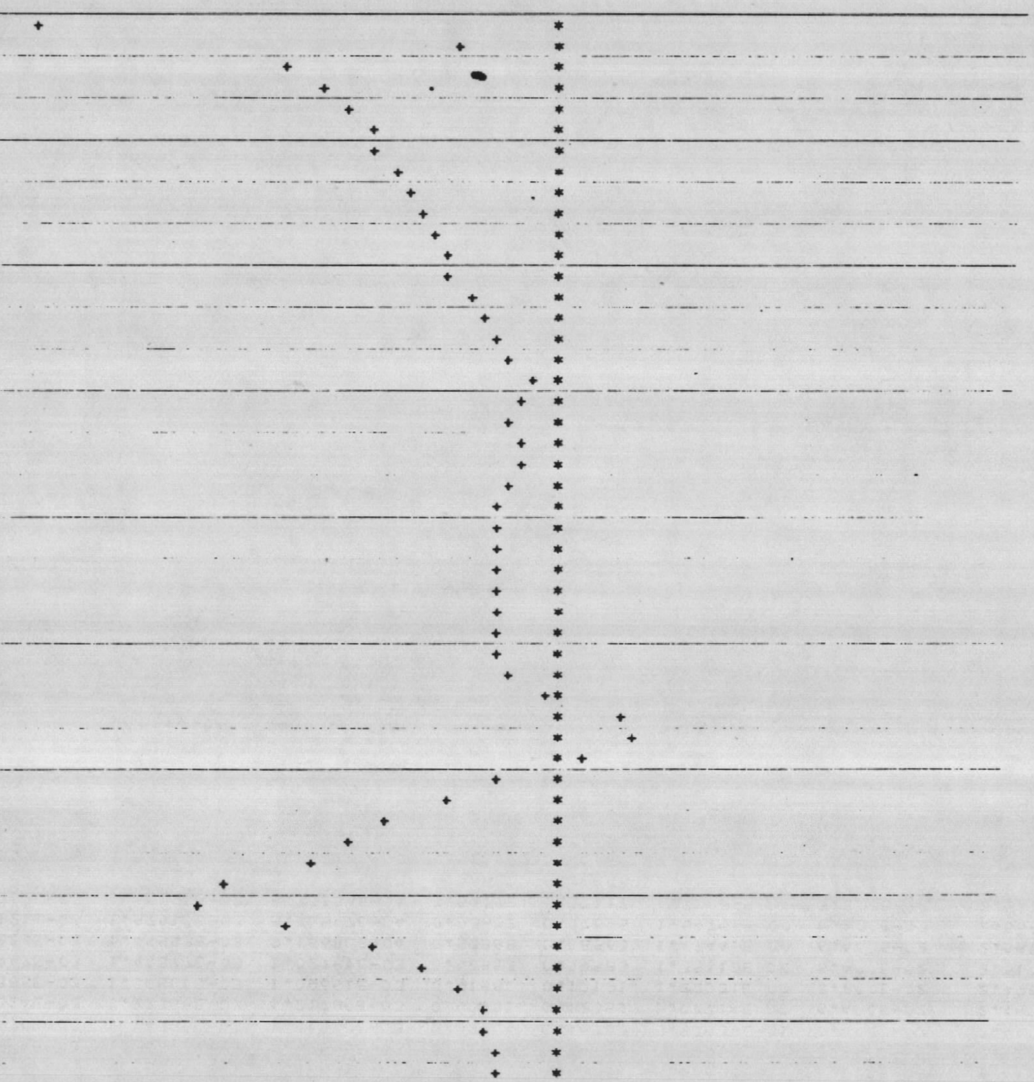

(e) The plot of C_p and list of M, u_e and C_p for inviscid flow on plain body.

Figure 6. Continued.

UZ = 1.19280E 04
REZ = 3.70060E 05

AX	UTAU	DELTA	DELST	THETA	CF	UE/UZ	CP	DELST+R	DX	HTR
2.00000E 00	2.68563E 02	6.71285E-03	2.69265E-03	9.76996E-04	1.46592E-03	0.85012	0.22004	6.42693E-01	1.000E-03	2.4467
2.52496E 00	2.72938E 02	7.29418E-03	2.92594E-03	1.06272E-03	1.42696E-03	0.87300	0.19176	7.89915E-01	3.200E-02	2.4226
3.03694E 00	2.68523E 02	7.86453E-03	3.19470E-03	1.14395E-03	1.31590E-03	0.89204	0.15363	9.33539E-01	6.400E-02	2.4406
3.54893E 00	2.63212E 02	8.42667E-03	3.46324E-03	1.22358E-03	1.21780E-03	0.90701	0.12350	1.07716E 00	6.400E-02	2.4603
4.06090E 00	2.53447E 02	9.03797E-03	3.77385E-03	1.30801E-03	1.09661E-03	0.91880	0.10191	1.22031E 00	3.200E-02	2.4983
4.61289E 00	2.48350E 02	9.70745E-03	4.08447E-03	1.40377E-03	1.02781E-03	0.92863	0.09585	1.35118E 00	6.400E-02	2.5103
5.12487E 00	2.35863E 02	1.03855E-02	4.43833E-03	1.49593E-03	9.15680E-04	0.93368	0.08563	1.47441E 00	6.400E-02	2.5570
5.63686E 00	2.31195E 02	1.09444E-02	4.70121E-03	1.57510E-03	8.70547E-04	0.93802	0.07695	1.59755E 00	6.400E-02	2.5694
6.14985E 00	2.32582E 02	1.14517E-02	4.90312E-03	1.65195E-03	6.73154E-04	0.94172	0.07117	1.71839E 00	3.200E-02	2.5492
6.66[illegible]84E 00	3.57319E 02	1.27993E-02	4.39494E-03	1.87293E-03	2.04347E-03	0.94522	0.06848	1.83308E 00	3.200E-02	1.9773
7.18883E 00	4.39557E 02	1.78699E-02	4.78825E-03	2.37462E-03	3.05230E-03	0.95062	0.05697	1.95227E 00	3.200E-02	1.6535
7.70082E 00	4.69800E 02	2.45333E-02	5.62169E-03	2.95961E-03	3.42341E-03	0.95826	0.04122	2.06830E 00	6.400E-02	1.5150
8.21281E 00	4.79195E 02	3.12605E-02	6.59442E-03	3.55605E-03	3.49758E-03	0.96588	0.02722	2.18235E 00	6.400E-02	1.4482
8.72480E 00	4.84285E 02	3.74146E-02	7.53022E-03	4.10252E-03	3.49166E-03	0.97550	0.00985	2.29336E 00	6.400E-02	1.4101
9.23680E 00	4.87470E 02	4.29697E-02	8.42740E-03	4.60798E-03	3.45382E-03	0.98569	-0.01078	2.40434E 00	1.280E-01	1.3869
9.74879E 00	4.90245E 02	4.80862E-02	9.27731E-03	5.07672E-03	3.41135E-03	0.99584	-0.03134	2.51527E 00	1.280E-01	1.3707
1.02608E 01	4.87799E 02	5.31998E-02	1.02447E-02	5.60343E-03	3.33375E-03	1.00143	-0.03657	2.61718E 00	6.400E-02	1.3631
1.07728E 01	4.85837E 02	5.83553E-02	1.11869E-02	6.12058E-03	3.27255E-03	1.00594	-0.04019	2.71029E 00	1.280E-01	1.3553
1.14123E 01	4.84644E 02	6.45456E-02	1.22874E-02	6.72467E-03	3.21439E-03	1.01158	-0.05157	2.82658E 00	2.560E-01	1.3461
1.19248E 01	4.84074E 02	6.93045E-02	1.31271E-02	7.18426E-03	3.17512E-03	1.01589	-0.06029	2.91958E 00	2.560E-01	1.3397
1.24368E 01	4.83749E 02	7.41005E-02	1.39656E-02	7.64247E-03	3.13998E-03	1.02015	-0.06387	3.00385E 00	2.560E-01	1.3337
1.29488E 01	4.83717E 02	7.87745E-02	1.47774E-02	8.08446E-03	3.10915E-03	1.02440	-0.07164	3.08658E 00	2.560E-01	1.3282
1.34607E 01	4.85307E 02	8.32891E-02	1.55109E-02	8.48154E-03	3.09072E-03	1.02988	-0.08270	3.16923E 00	3.200E-02	1.3216
1.40367E 01	4.91687E 02	8.80079E-02	1.61392E-02	8.81134E-03	3.09777E-03	1.04038	-0.10334	3.26091E 00	1.280E-01	1.3108
1.45487E 01	4.96532E 02	9.22956E-02	1.67733E-02	9.13611E-03	3.09361E-03	1.04966	-0.11502	3.32811E 00	1.280E-01	1.3034
1.51887E 01	5.02228E 02	9.73568E-02	1.75599E-02	9.52873E-03	3.08409E-03	1.06120	-0.13839	3.41209E 00	2.560E-01	1.2960
1.57007E 01	4.93871E 02	1.01711E-01	1.88447E-02	1.01924E-02	2.98915E-03	1.06018	-0.13661	3.47994E 00	1.280E-01	1.3057
1.62127E 01	4.85672E 02	1.06524E-01	2.00532E-02	1.08421E-02	2.91566E-03	1.05634	-0.12390	3.53600E 00	2.560E-01	1.3115
1.67245E 01	4.78426E 02	1.12021E-01	2.13050E-02	1.15254E-02	2.85382E-03	1.05250	-0.11079	3.57565E 00	2.560E-01	1.3149
1.72366E 01	4.72088E 02	1.17655E-01	2.25165E-02	1.21965E-02	2.80288E-03	1.04865	-0.10301	3.61526E 00	2.560E-01	1.3167
1.77486E 01	4.65305E 02	1.23438E-01	2.37848E-02	1.29009E-02	2.75184E-03	1.04397	-0.09353	3.65493E 00	5.120E-01	1.3190
1.82606E 01	4.58932E 02	1.29307E-01	2.50216E-02	1.35993E-02	2.70793E-03	1.03889	-0.08332	3.69455E 00	5.120E-01	1.3204
1.87726E 01	4.53043E 02	1.35253E-01	2.62387E-02	1.42941E-02	2.66958E-03	1.03379	-0.07305	3.73418E 00	5.120E-01	1.3210
1.92846E 01	4.47566E 02	1.41271E-01	2.74377E-02	1.49856E-02	2.63591E-03	1.02868	-0.06276	3.77378E 00	5.120E-01	1.3211
1.97964E 01	4.45594E 02	1.47308E-01	2.84439E-02	1.55723E-02	2.62265E-03	1.02702	-0.05936	3.81317E 00	6.400E-02	1.3173
2.03083E 01	4.50890E 02	1.53011E-01	2.88617E-02	1.58450E-02	2.65607E-03	1.03183	-0.06742	3.84582E 00	1.280E-01	1.3043
2.08202E 01	4.55363E 02	1.58565E-01	2.93512E-02	1.61399E-02	2.67964E-03	1.03663	-0.07626	3.87445E 00	2.560E-01	1.2938
2.13322E 01	4.59289E 02	1.63861E-01	2.98692E-02	1.64374E-02	2.69663E-03	1.04142	-0.08590	3.90314E 00	2.560E-01	1.2852
2.18441E 01	4.62814E 02	1.68931E-01	3.04059E-02	1.67355E-02	2.70880E-03	1.04620	-0.09552	3.93183E 00	1.280E-01	1.2779
2.24199E 01	4.61593E 02	1.74685E-01	3.14232E-02	1.72984E-02	2.69074E-03	1.04682	-0.09616	3.96032E 00	1.280E-01	1.2765
2.30598E 01	4.59229E 02	1.81200E-01	3.26561E-02	1.79823E-02	2.66532E-03	1.04647	-0.09525	3.99035E 00	2.560E-01	1.2761
2.35718E 01	4.57511E 02	1.86419E-01	3.36243E-02	1.85213E-02	2.64706E-03	1.04620	-0.09469	4.01435E 00	2.560E-01	1.2755
2.40837E 01	4.55897E 02	1.91803E-01	3.46053E-02	1.90695E-02	2.63006E-03	1.04592	-0.09357	4.03461E 00	2.560E-01	1.2748
2.45957E 01	4.51767E 02	1.98007E-01	3.59046E-02	1.98046E-02	2.59983E-03	1.04298	-0.08626	4.03590E 00	2.560E-01	1.2764
2.51076E 01	4.44689E 02	2.04560E-01	3.75735E-02	2.07438E-02	2.55170E-03	1.03729	-0.07481	4.03757E 00	1.280E-01	1.2819
2.56195E 01	4.38021E 02	2.11362E-01	3.92424E-02	2.16904E-02	2.50809E-03	1.03157	-0.06332	4.03924E 00	2.560E-01	1.2865
2.61315E 01	4.31702E 02	2.18381E-01	4.09147E-02	2.26459E-02	2.46829E-03	1.02585	-0.05181	4.04091E 00	2.560E-01	1.2906
2.66434E 01	4.25682E 02	2.25596E-01	4.25940E-02	2.36121E-02	2.43170E-03	1.02010	-0.04028	4.04259E 00	2.560E-01	1.2941
2.71553E 01	4.21617E 02	2.32964E-01	4.41079E-02	2.44911E-02	2.40696E-03	1.01620	-0.03244	4.04411E 00	1.280E-01	1.2950
2.76672E 01	4.18853E 02	2.40259E-01	4.5432[illegible]E-02	2.52763E-02	2.39138E-03	1.01321	-0.02646	4.04543E 00	2.560E-01	1.2940
2.81792E 01	4.16136E 02	2.47581E-01	4.67608E-02	2.60662E-02	2.37728E-03	1.01022	-0.02047	4.04676E 00	2.560E-01	1.2930
2.86911E 01	4.13462E 02	2.54929E-01	4.80939E-02	2.68611E-02	2.36311E-03	1.00723	-0.01447	4.04809E 00	2.560E-01	1.2921
2.92031E 01	4.10828E 02	2.62302E-01	4.94317E-02	2.76612E-02	2.34935E-03	1.00423	-0.00847	4.04943E 00	2.560E-01	1.2912
2.97150E 01	4.10983E 02	2.69468E-01	5.03367E-02	2.82298E-02	2.35320E-03	1.00385	-0.00770	4.05034E 00	1.280E-01	1.2863

(f) First part of boundary-layer calculation for first iteration.

Figure 6. Continued.

AX	UTAU	DELTA	DELST	THETA	CF	UE/UZ	CP	DELST+R	DX	HTR
5.20173E 01	5.35965E 02	5.57019E-01	6.59949E-02	3.51564E-02	2.76287E-03	1.17182	-0.35502	3.97844E 00	1.000E-03	1.0766
5.25248E 01	5.36599E 02	5.65117E-01	6.78392E-02	3.60542E-02	2.74569E-03	1.17590	-0.36810	3.91640E 00	6.400E-02	1.0785
5.30524E 01	5.20678E 02	5.68178E-01	7.24852E-02	3.89540E-02	2.66931E-03	1.16075	-0.34555	3.83566E 00	3.200E-02	1.0967
5.35963E 01	4.80872E 02	5.70203E-01	8.24545E-02	4.53801E-02	2.49454E-03	1.11813	-0.26795	3.73713E 00	6.400E-02	1.1398
5.41080E 01	4.40021E 02	5.82833E-01	9.52423E-02	5.32540E-02	2.29838E-03	1.07449	-0.18971	3.62899E 00	1.600E-02	1.1851
5.46519E 01	3.79082E 02	6.11549E-01	1.19747E-01	6.73992E-02	1.97461E-03	1.00982	-0.06500	3.50361E 00	6.400E-02	1.2676
5.51638E 01	3.18688E 02	6.61400E-01	1.55679E-01	8.61540E-02	1.61232E-03	0.94860	0.05401	3.37839E 00	1.280E-01	1.3715
5.56757E 01	2.57453E 02	7.39506E-01	2.11542E-01	1.11709E-01	1.21253E-03	0.89109	0.16909	3.25259E 00	6.400E-02	1.5164

AX	UTAU	DELTA	DELST	THETA	CF	UE/UZ	CP	DELST+R	DX	HTR
5.56757E 01	0.0	3.76784E-01	2.11541E-01	4.71460E-02	0.0	0.89077	0.16973	3.25259E 00	6.400E-02	4.0000
5.61875E 01	-5.63030E 01	5.14232E-01	3.21433E-01	5.32324E-02	-5.90893E-05	0.88368	0.20416	3.15964E 00	6.400E-02	5.5049
5.66994E 01	-8.37514E 01	6.62511E-01	4.48954E-01	5.77083E-02	-1.30281E-04	0.88509	0.20119	3.06629E 00	6.400E-02	7.2396
5.72112E 01	-9.65271E 01	8.09397E-01	5.83761E-01	6.33397E-02	-1.72306E-04	0.88681	0.19797	2.97322E 00	6.400E-02	8.7091
5.77232E 01	-1.00711E 02	9.46742E-01	7.19458E-01	7.16504E-02	-1.88204E-04	0.88547	0.20050	2.87996E 00	6.400E-02	9.5817
5.82350E 01	-9.06416E 01	1.02045E 00	7.86809E-01	8.74200E-02	-1.55877E-04	0.87674	0.21764	2.78681E 00	3.200E-02	8.5244
5.85549E 01	-7.45656E 01	9.79890E-01	7.28564E-01	9.69123E-02	-1.09124E-04	0.86356	0.24335	2.72858E 00	6.400E-02	7.0363

AX	UTAU	DELTA	DELST	THETA	CF	UE/UZ	CP	DELST+R	DX	HTR
5.85549E 01	7.13804E 01	1.22438E 00	7.28556E-01	2.27754E-01	9.99998E-05	0.86356	0.24333	2.72856E 00	6.400E-04	2.8025
5.90693E 01	1.85170E 02	1.03030E 00	4.34838E-01	1.94343E-01	6.12914E-04	0.90029	-0.03632	2.43484E 00	4.096E-02	1.8475
5.95754E 01	2.06619E 02	1.01848E 00	4.00484E-01	1.87887E-01	7.46471E-04	0.90913	0.17605	2.40048E 00	8.192E-02	1.7768
6.00873E 01	2.35715E 02	1.00008E 00	3.57234E-01	1.76613E-01	9.30668E-04	0.92653	0.13995	2.35723E 00	2.048E-02	1.6142
6.05991E 01	2.56864E 02	9.92669E-01	3.29976E-01	1.68501E-01	1.06884E-03	0.94023	0.11642	2.32998E 00	8.192E-02	1.5373
6.11725E 01	2.81848E 02	9.84989E-01	3.00783E-01	1.58332E-01	1.22994E-03	0.95902	0.07946	2.30078E 00	1.638E-01	1.4595
6.18276E 01	2.93697E 02	9.90557E-01	2.89499E-01	1.54600E-01	1.31049E-03	0.96695	0.06563	2.28950E 00	1.638E-01	1.4232
6.24830E 01	3.05552E 02	9.96118E-01	2.78666E-01	1.50657E-01	1.38921E-03	0.97573	0.04820	2.27867E 00	1.638E-01	1.3897
6.31382E 01	3.16922E 02	1.00202E 00	2.68807E-01	1.46799E-01	1.46298E-03	0.98478	0.03020	2.26881E 00	3.277E-01	1.3599
6.37935E 01	3.21217E 02	1.01156E 00	2.66090E-01	1.46113E-01	1.49534E-03	0.98693	0.02610	2.26609E 00	1.638E-01	1.3462
6.41212E 01	3.23010E 02	1.01650E 00	2.65132E-01	1.45928E-01	1.50908E-03	0.98778	0.02442	2.26513E 00	1.638E-01	1.3404

STATUS OF ITERATION

XMAX = 62.0000
DPMAX = 0.1434E 00
DSMAX = 0.2868E 00

INPUT VALUES FOR RESTART ARE

LPROG = 0
NRSTRT = 1
NPRINT = 0
N1MAX = 7
N1 = 2
N2 = 1
N3 = 1
IBL = 3
MIT2 = 20

(g) End of first boundary-layer calculation.

Figure 6. Continued.

COMPARISON OF VISCOUS AND INVISCID VELOCITIES IN SEPARATED REGION

+ = BOUNDARY LAYER
0 = INVISCID SOLUTION

X	UEBL	UEINV	0.3 UE/UZ 1.0
55.093	0.90846	0.90388	0
56.511	0.90773	0.90003	0
56.929	0.90900	0.89806	0+
57.347	0.90960	0.89912	0+
57.764	0.90810	0.92950	+0
58.192	0.89854	0.92769	+ 0
58.600	0.88300	0.89030	+0
59.016	0.86605	0.87554	+0
59.436	0.85063	0.86189	+0
59.853	0.83753	0.84686	+0
60.271	0.83819	0.85120	+0
60.689	0.84370	0.85901	+0
61.107	0.85130	0.86692	+0
61.524	0.86065	0.87568	+0
61.942	0.87048	0.88464	0
62.360	0.88052	0.89360	+0
62.778	0.89063	0.90256	+0
63.195	0.90035	0.91142	0
63.613	0.90781	0.91716	+0

INTERMEDIATE RESULTS OF THETA ITERATION

DTHET = 0.0
DIFFS = 0.38587E-02

FIRST BOUNDARY LAYER FOR ITERATION 6 FOLLOWS.

INPUT VALUES FOR RESTART ARE

LPROG	= 0
NRSTRT	= 1
NPRINT	= 0
N1MAX	= 7
N1	= 5
N2	= 2
N3	= 1
IBL	= 0
MIT2	= 30

(h) Comparison of viscous and inviscid velocities for initial value of θ_s; N1 = 3, N2 = 1, and N3 = 1.

Figure 6. Continued.

```
COMPARISON OF VISCOUS AND INVISCID VELOCITIES IN SEPARATED REGION

      + = BOUNDARY LAYER
      O = INVISCID SOLUTION

   X        UEBL      UEINV   0.3              UE/UZ                   1.0
 56.100   0.91484   0.91119                                            O
 56.524   0.91191   0.90198                                            O
 56.949   0.91045   0.88965                                           O+
 57.373   0.90868   0.87120                                          O +
 57.798   0.90542   0.90676                                            O
 58.222   0.89684   0.89340                                           O
 58.646   0.87717   0.85260                                        O +
 59.071   0.85979   0.83431                                       O +
 59.495   0.84757   0.82333                                      O +
 59.920   0.84329   0.81307                                      O +
 60.344   0.85058   0.82777                                       O+
 60.768   0.86178   0.84247                                        O+
 61.193   0.87395   0.85685                                         O+
 61.617   0.88511   0.86887                                         O +
 62.042   0.89567   0.88090                                          O+
 62.466   0.90603   0.89293                                           O+
 62.890   0.91630   0.90495                                            O+
 63.315   0.92383   0.91497                                            O+
 63.739   0.92867   0.92656                                             O

INTERMEDIATE RESULTS OF THETA ITERATION

 DTHET  =     1.5000
 DIFFS  =   0.681895E-02

FINAL RESULTS OF THETA ITERATION

 XSEP   =   55.5757
 DTHET  =   1.00
 DIFFS  =  0.25489E-02

  FIRST BOUNDARY LAYER FOR ITERATION  12 FOLLOWS.

       INPUT VALUES FOR RESTART ARE

              LPROG    = 0
              NRSTRT   = 1
              NPRINT   = 0
              N1MAX    =  7
              N1       = 11
              N2       =  1
              N3       =  2
              IBL      =  0
              MIT2     = 30
```

(i) Comparison of viscous and inviscid velocities for an intermediate iteration; N1 = 4, N2 = 2, and N3 = 1.

Figure 6. Continued.

COMPARISON OF VISCOUS AND INVISCID VELOCITIES IN SEPARATED REGION

+ = BOUNDARY LAYER
O = INVISCID SOLUTION

X	UEBL	UEINV	0.3 UE/UZ 1.0
55.723	0.93272	0.93254	O
56.165	0.93008	0.92758	O+
56.606	0.93091	0.92388	O+
57.048	0.93159	0.91294	O +
57.489	0.93061	0.90727	O +
57.931	0.92688	0.93544	+O
58.372	0.91373	0.90472	O
58.814	0.89164	0.87923	O+
59.255	0.87299	0.86484	O+
59.697	0.85678	0.84917	O+
60.138	0.85205	0.84641	O
60.580	0.85773	0.85648	O
61.021	0.86642	0.86656	O
61.463	0.87457	0.87528	O
61.904	0.88252	0.88302	O
62.346	0.89047	0.89095	O
62.787	0.89842	0.89889	O
63.228	0.90591	0.90664	O
63.670	0.91241	0.91274	O

INTERMEDIATE RESULTS OF THETA ITERATION

DTHET = 2.5000
DIFFS = 0.13710E-02

FIRST BOUNDARY LAYER FOR ITERATION 21 FOLLOWS.

INPUT VALUES FOR RESTART ARE

LPROG = 0
NRSTRT = 1
NPRINT = 0
N1MAX = 7
N1 = 20
N2 = 5
N3 = 3
IBL = 0
MIT2 = 30

(j) Comparison of viscous and inviscid velocities at iteration 17.

Figure 6. Continued.

PLOT OF CP AT EQUAL XI-INCREMENTS

I	XB	YB	FM	QS	CP
1	0.0	0.0	0.0	0.0	1.2192
2	0.193	0.062	0.878	0.979	0.0424
3	0.404	0.130	0.611	0.706	0.5540
4	0.650	0.209	0.678	0.777	0.4296
5	0.948	0.305	0.708	0.809	0.3707
6	1.315	0.422	0.731	0.832	0.3272
7	1.764	0.568	0.762	0.864	0.2670
8	2.312	0.736	0.797	0.899	0.1993
9	2.977	0.918	0.811	0.913	0.1722
10	3.770	1.114	0.811	0.913	0.1723
11	4.696	1.338	0.812	0.914	0.1699
12	5.761	1.596	0.826	0.928	0.1429
13	6.971	1.890	0.855	0.957	0.0863
14	8.333	2.198	0.882	0.983	0.0348
15	9.853	2.499	0.892	0.992	0.0155
16	11.523	2.812	0.916	1.015	-0.0304
17	13.342	3.118	0.954	1.051	-0.1022
18	15.306	3.377	0.965	1.062	-0.1238
19	17.404	3.596	0.968	1.064	-0.1277
20	19.621	3.780	0.977	1.072	-0.1446
21	21.942	3.910	0.975	1.070	-0.1407
22	24.347	3.999	0.965	1.061	-0.1225
23	26.817	4.035	0.946	1.044	-0.0879
24	29.328	4.049	0.929	1.028	-0.0554
25	31.858	4.055	0.921	1.020	-0.0399
26	34.383	4.060	0.917	1.016	-0.0324
27	36.877	4.064	0.914	1.014	-0.0275
28	39.314	4.068	0.915	1.014	-0.0285
29	41.670	4.072	0.920	1.019	-0.0381
30	43.919	4.075	0.926	1.025	-0.0497
31	46.038	4.075	0.937	1.035	-0.0700
32	48.005	4.067	0.955	1.052	-0.1037
33	49.801	4.040	0.968	1.064	-0.1291
34	51.411	3.997	1.079	1.163	-0.3301
35	52.825	3.863	1.204	1.255	-0.5408
36	54.036	3.634	1.060	1.125	-0.2964
37	55.046	3.423	0.874	0.953	0.0504
38	55.864	3.252	0.848	0.931	0.0997
39	56.507	3.127	0.845	0.930	0.1051
40	57.004	3.030	0.834	0.918	0.1263
41	57.394	2.952	0.812	0.898	0.1703
42	57.730	2.895	0.842	0.933	0.1109
43	58.080	2.835	0.855	0.937	0.0866
44	58.517	2.736	0.805	0.887	0.1842
45	59.100	2.629	0.781	0.868	0.2307
46	59.917	2.479	0.748	0.837	0.2940
47	61.141	2.308	0.761	0.861	0.2681
48	63.182	2.218	0.806	0.907	0.1818
49	67.264	2.186	0.863	0.965	0.0705
50	79.509	2.186	0.895	0.995	0.0093
51	********	2.186	0.900	1.000	0.0

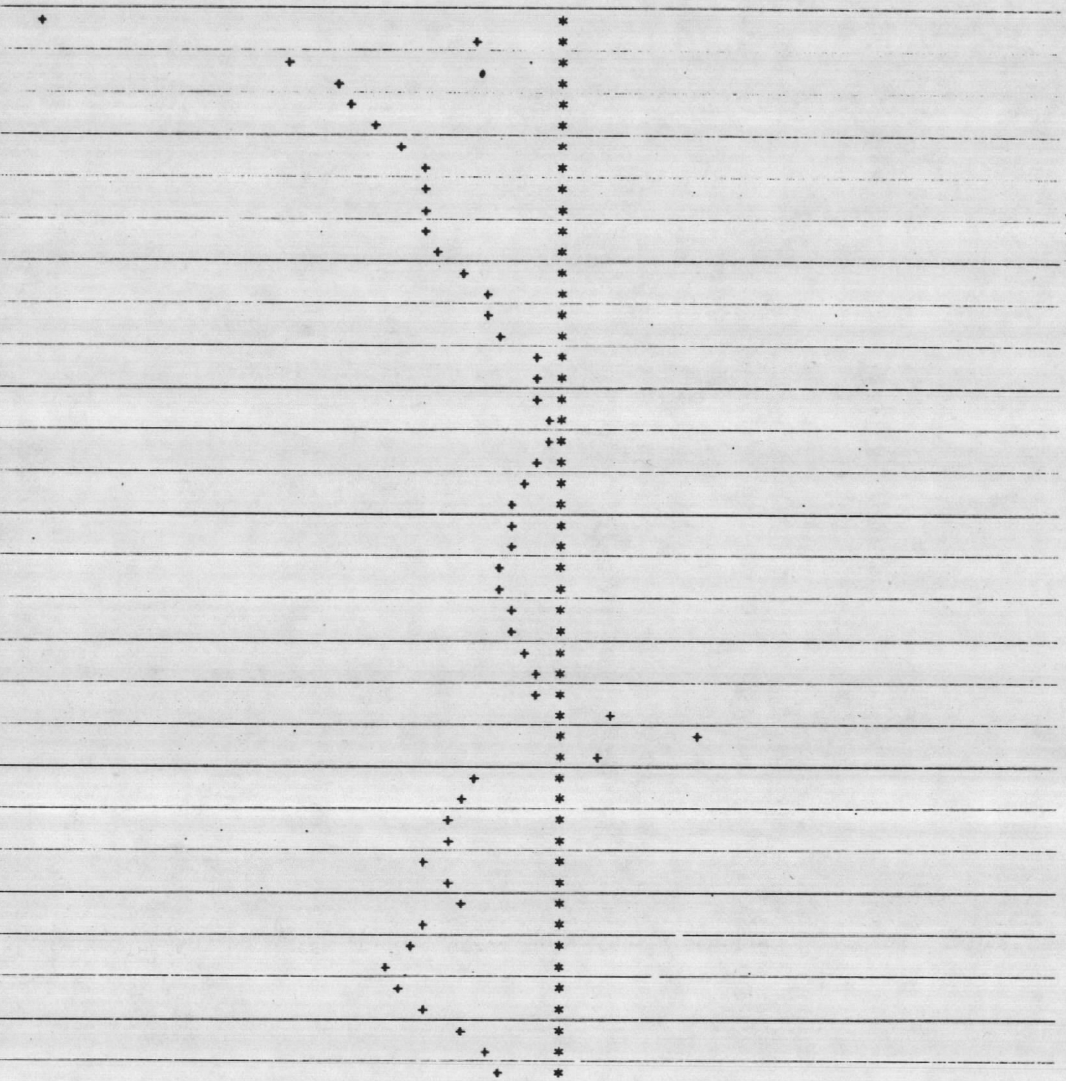

(k) Final C_p plot and list of M, u_e and C_p.

Figure 6. Continued.

DRAG COEFFICIENT BY TRAPEZOIDAL INTEGRATION= 0.04654

DRAG COEFFICIENT BY SIMPSON INTEGRATION= 0.04786

COMPUTING TIME= 552.3 SECONDS

AX	UTAU	DELTA	DELST	THETA	CF	UE/UZ	CP	DELST+R	DX	HTR
5.20495E 01	5.59413E 02	5.59796E-01	6.49148E-02	3.37496E-02	2.80634E-03	1.20524	-0.41408	3.97337E 00	6.711E-02	1.0655
5.25863E 01	5.85340E 02	5.84805E-01	6.41407E-02	3.24024E-02	2.86178E-03	1.23961	-0.49723	3.90297E 00	6.711E-02	1.0437
5.31059E 01	5.69535E 02	5.81756E-01	6.83982E-02	3.50682E-02	2.78970E-03	1.22541	-0.47622	3.82123E 00	3.355E-02	1.0635
5.36428E 01	5.16242E 02	5.68951E-01	7.88383E-02	4.21310E-02	2.58371E-03	1.16806	-0.36965	3.72297E 00	6.711E-02	1.1185
5.41460E 01	4.59066E 02	5.73086E-01	9.35532E-02	5.13871E-02	2.33017E-03	1.10679	-0.25505	3.61725E 00	1.678E-02	1.1807
5.46828E 01	3.72941E 02	6.01466E-01	1.25450E-01	6.94607E-02	1.88169E-03	1.01656	-0.07417	3.49998E 00	6.711E-02	1.2972
5.51980E 01	3.04021E 02	6.58624E-01	1.68167E-01	9.05934E-02	1.46553E-03	0.94910	0.05687	3.37920E 00	3.355E-02	1.4252
5.52987E 01	3.01374E 02	6.67680E-01	1.71764E-01	9.24485E-02	1.44942E-03	0.94644	0.03217	3.34846E 00	3.355E-02	1.4295

AX	UTAU	DELTA	DELST	THETA	CF	UE/UZ	CP	DELST+R	DX	HTR
5.52819E 01	0.0	3.06037E-01	1.71165E-01	3.73965E-02	0.0	0.94686	0.03130	3.35357E 00	3.355E-02	4.0000
5.58018E 01	-5.78567E 01	4.23130E-01	2.60130E-01	4.33707E-02	-5.51507E-05	0.93329	0.10262	3.25314E 00	6.711E-02	5.3655
5.63386E 01	-9.05722E 01	5.62165E-01	3.74595E-01	4.74731E-02	-1.35461E-04	0.93236	0.10417	3.14893E 00	6.711E-02	7.2265
5.68419E 01	-1.05886E 02	7.025685E-01	4.96943E-01	5.21144E-02	-1.84172E-04	0.93451	0.09964	3.05085E 00	6.711E-02	8.8870
5.74458E 01	-1.12570E 02	8.63570E-01	6.48044E-01	5.98925E-02	-2.08632E-04	0.93357	0.10148	2.93307E 00	1.342E-01	10.2299
5.79827E 01	-1.11680E 02	9.97076E-01	7.84865E-01	7.05767E-02	-2.07655E-04	0.92900	0.11076	2.82864E 00	1.342E-01	10.5716
5.84857E 01	-9.07604E 01	9.62099E-01	7.30863E-01	8.45488E-02	-1.44239E-04	0.90856	0.15147	2.73086E 00	6.711E-02	8.0658
5.90897E 01	-5.20339E 01	8.77759E-01	6.13480E-01	1.01580E-01	-5.07355E-05	0.88161	0.20466	2.61348E 00	1.342E-01	5.5181
5.95929E 01	-5.13952E 00	8.10072E-01	5.15666E-01	1.14023E-01	-5.20658E-07	0.86189	0.24319	2.51567E 00	3.355E-02	4.0734
5.99620E 01	4.19190E 01	7.62702E-01	4.43933E-01	1.20669E-01	3.56181E-05	0.85115	0.26406	2.44393E 00	6.711E-02	3.2802

AX	UTAU	DELTA	DELST	THETA	CF	UE/UZ	CP	DELST+R	DX	HTR
5.99620E 01	7.02385E 01	8.05233E-01	4.43916E-01	1.36991E-01	9.99999E-05	0.85115	0.26405	2.44392E 00	6.711E-04	2.8579
6.04871E 01	1.33311E 02	7.44454E-01	3.44511E-01	1.34265E-01	3.56079E-04	0.85559	0.25684	2.34451E 00	4.295E-02	2.2059
6.10023E 01	1.71052E 02	7.22802E-01	2.97697E-01	1.29663E-01	5.73944E-04	0.86376	0.26116	2.29770E 00	8.590E-02	1.9382
6.15605E 01	2.03921E 02	7.09927E-01	2.62464E-01	1.23820E-01	7.91834E-04	0.87532	0.24212	2.26246E 00	8.590E-02	1.7565
6.20757E 01	2.28664E 02	7.04268E-01	2.39148E-01	1.18663E-01	9.67368E-04	0.88663	0.22175	2.23915E 00	1.718E-01	1.6436
6.25911E 01	2.49515E 02	7.02343E-01	2.21492E-01	1.13983E-01	1.11958E-03	0.89790	0.20060	2.22149E 00	1.718E-01	1.5614
6.31064E 01	2.67715E 02	7.02666E-01	2.07439E-01	1.09710E-01	1.25333E-03	0.90909	0.17916	2.20744E 00	1.718E-01	1.4978
6.36644E 01	2.80979E 02	7.07309E-01	1.98438E-01	1.06938E-01	1.35349E-03	0.91709	0.16392	2.19844E 00	8.590E-02	1.4536
6.40079E 01	2.88118E 02	7.10716E-01	1.93892E-01	1.05467E-01	1.40733E-03	0.92162	0.15513	2.19389E 00	1.718E-01	1.4311

STATUS OF ITERATION

XMAX = 60.0000
DPMAX = 0.1673E-01
DSMAX = 0.4313E 00

****ITERATION FOR BOUNDARY LAYER/INVISCID FLOW EQUILIBRIUM CONVERGED

(1) Final list of boundary-layer quantities.

Figure 6. Concluded.

```
BLAHA,CHAMBERLIN AND BOBER  6524  BOATTAIL-STING
TESTING COMPLETE ITERATION
TRANSONIC FLOW WITH WEAK SHOCK ON AFTERBODY   RESTARTING AFTER 4 ITERATIONS
    0    1    0    7    4    1    1    3   30
```


Figure 7.- Input data for restarting calculation of viscid-inviscid interaction after 4 iterations.

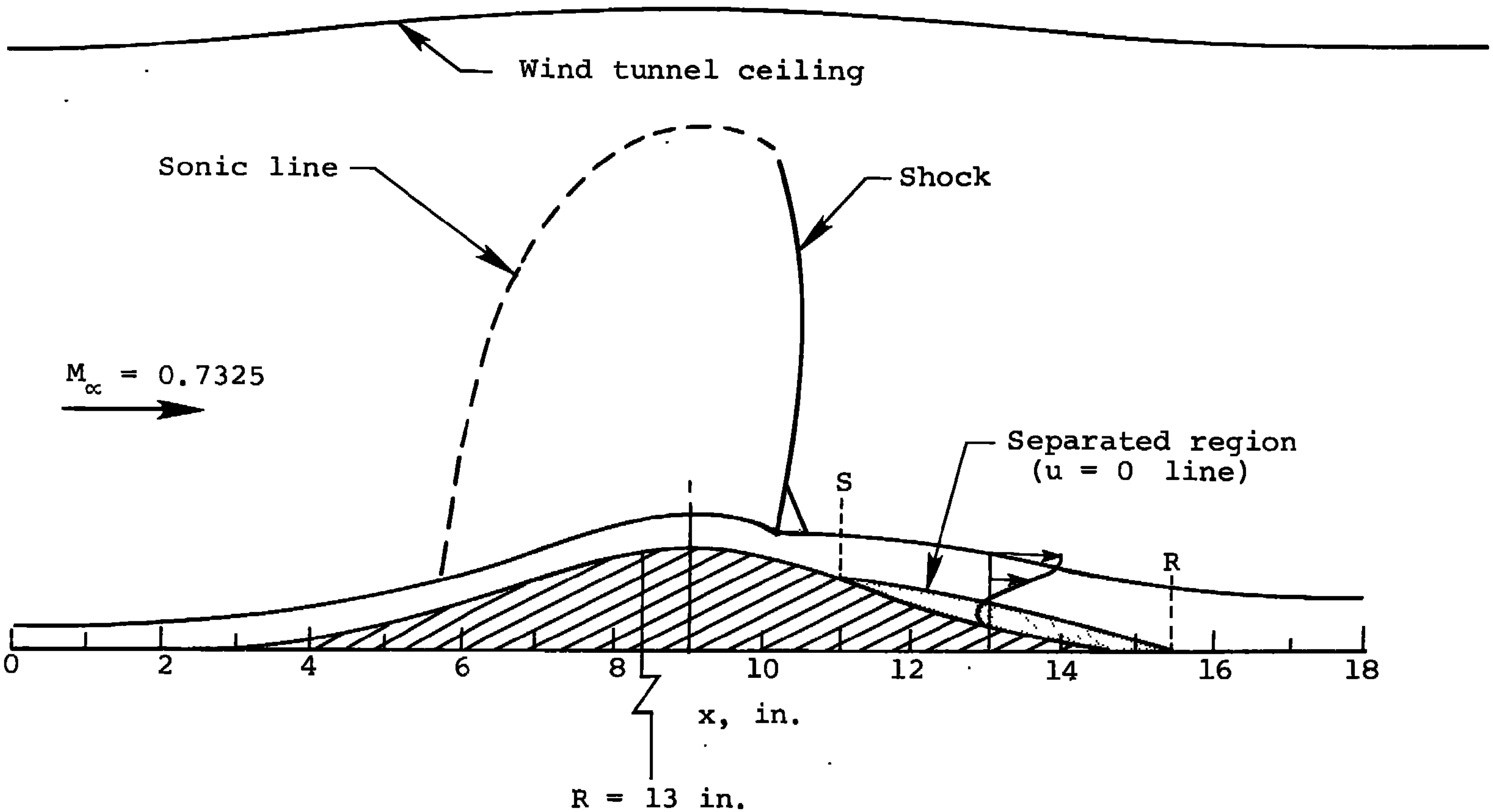

Figure 8. Two-dimensional configuration for boundary-layer calculation.

```
          ALBER TEST CASE
 TWO-DIMENSIONAL BOUNDARY LAYER CALCULATION
 SPECIFYING VELOCITY DISTRIBUTION FROM X=0
 1
 1.4      .7325
 1    0    0    0    2    0    2    0
22
 0.0     9750.
 1.0     9480.
 2.0     9400.
 3.0     8500.
 4.0     8650.
 5.0     9750.
 6.0    11650.
 7.0    12980.
 8.0    14200.
 9.0    15480.
10.0    16100.
10.25   14800.
10.75   13400.
11.0    12600.
11.50   12100.
12.0    11150.
13.0    10900.
14.0    10800.
15.0    10300.
16.0     9900.
17.0     9800.
18.0    10200.
 1.0     15.0    585.0     .99     0.0     0.0     0.0     0.0
 0.0     15.0     -5.0    .001    0.0     0.5
.00233   .065
19
 0.0      0.0
 1.0      0.0
 2.0      0.0
 3.0      0.0
 4.0      0.25
 5.0      0.50
 6.0      0.70
 7.0      0.85
 8.0      0.98
 9.0      1.0
10.0      0.98
11.0      0.85
12.0      0.70
13.0      0.50
14.0      0.25
15.0      0.0
16.0      0.0
17.0      0.0
18.0      0.0
```

(a) Input for case with u_e specified.

Figure 9. Input data for two-dimensional boundary-layer calculation.

```
          ALBER TEST CASE
 TWO-DIMENSIONAL BOUNDARY LAYER CALCULATION
 SPECIFYING DELST DISTRIBUTION FROM X=10.75
 1
 1.4       .7325
 2    0    0    0    2    0    2    0
13
10.0      .03
10.25     .05
10.75     .07
11.0      .083
11.5      .112
12.0      .148
13.0      .314
14.0      .435
14.5      .460
15.0      .440
16.0      .306
17.0      .230
18.0      .190
 1.0      15.0      585.0      .99      0.0      0.0      0.0      0.0
10.75     18.0       -5.0     .001      0.0      0.5
.00077
13400.   -2820.
19
 0.0       0.0
 1.0       0.0
 2.0       0.0
 3.0       0.0
 4.0       0.25
 5.0       0.50
 6.0       0.70
 7.0       0.85
 8.0       0.98
 9.0       1.0
10.0       0.98
11.0       0.85
12.0       0.70
13.0       0.50
14.0       0.25
15.0       0.0
16.0       0.0
17.0       0.0
18.0       0.0
```

(b) Input data for case with δ^* specified.

Figure 9. Concluded.

UZ	=	9.90272E 03
REZ	=	3.02426E 05

AX	UTAU	DELTA	DELST	THETA	CF	UE/UZ	CP	DELST+R	DX	HTR
0.0	3.32242E 02	3.89870E-01	6.50011E-02	3.91983E-02	2.33000E-03	0.98458	0.03073	6.50011E-02	1.000E-03	1.2724
5.07999E-01	3.21451E 02	4.00204E-01	6.90991E-02	4.15509E-02	2.25014E-03	0.97076	0.05802	6.90991E-02	6.400E-02	1.2592
1.02000E 00	3.10897E 02	4.11624E-01	7.34969E-02	4.40558E-02	2.17112E-03	0.95715	0.08474	7.34969E-02	6.400E-02	1.3062
1.59598E 00	3.08014E 02	4.22195E-01	7.55501E-02	4.53285E-02	2.15394E-03	0.95250	0.09389	7.55501E-02	1.280E-01	1.3074
2.09994E 00	2.99019E 02	4.33894E-01	7.97424E-02	4.77122E-02	2.08831E-03	0.94026	0.11767	7.97424E-02	1.600E-02	1.3218
2.62793E 00	2.59825E 02	4.62968E-01	9.82106E-02	5.70932E-02	1.76648E-03	0.89244	0.20822	9.82106E-02	1.280E-01	1.4095
3.14789E 00	2.33328E 02	4.93046E-01	1.14806E-01	6.49474E-02	1.54092E-03	0.86059	0.26072	1.51780E-01	3.200E-02	1.4796
3.75588E 00	2.45922E 02	4.99273E-01	1.09046E-01	6.30893E-02	1.67291E-03	0.86980	0.20864	2.98015E-01	1.280E-01	1.4314
4.30764E 00	2.80790E 02	4.89843E-01	9.19850E-02	5.52319E-02	1.98671E-03	0.90808	0.14172	4.18945E-01	6.400E-02	1.3355
4.88383E 00	3.30543E 02	4.76783E-01	7.30426E-02	4.49303E-02	2.37327E-03	0.97186	0.01524	5.44000E-01	1.280E-01	1.2341
5.40379E 00	3.94375E 02	4.76848E-01	5.62893E-02	3.43779E-02	2.76443E-03	1.06362	-0.15988	6.37048E-01	6.400E-02	1.1383
5.97778E 00	4.64449E 02	4.98098E-01	4.46252E-02	2.59309E-02	3.07028E-03	1.17270	-0.39113	7.40581E-01	1.280E-01	1.0539
6.49177E 00	5.07260E 02	5.26895E-01	4.01207E-02	2.21274E-02	3.19517E-03	1.24345	-0.53033	8.13886E-01	1.280E-01	1.0071
7.00376E 00	5.46896E 02	5.73391E-01	3.72635E-02	1.92269E-02	3.27405E-03	1.31123	-0.67677	8.87753E-01	1.280E-01	0.9613
7.51576E 00	5.82820E 02	6.61514E-01	3.56100E-02	1.67643E-02	3.30934E-03	1.37522	-0.80889	9.52659E-01	1.280E-01	0.9054
8.03572E 00	6.19694E 02	3.60215E-01	3.44282E-02	1.72689E-02	3.34929E-03	1.43873	-0.94256	1.01514E 00	6.400E-02	1.0507
8.54772E 00	6.64967E 02	3.77848E-01	3.32710E-02	1.57975E-02	3.43576E-03	1.50590	-1.06694	1.02423E 00	6.400E-02	1.0231
9.05971E 00	7.07950E 02	3.96316E-01	3.21225E-02	1.43716E-02	3.51256E-03	1.56701	-1.19331	1.03093E 00	1.280E-01	0.9961
9.57170E 00	7.28438E 02	3.92213E-01	3.26993E-02	1.43427E-02	3.52377E-03	1.59929	-1.25931	1.02127E 00	6.400E-02	0.9990
1.00757E 01	7.15223E 02	3.57844E-01	3.42183E-02	1.54963E-02	3.46641E-03	1.58716	-1.23561	1.00438E 00	8.000E-03	1.0344
1.06276E 01	5.44701E 02	2.95032E-01	4.60271E-02	2.38717E-02	2.82507E-03	1.38871	-0.83271	9.44434E-01	6.400E-02	1.1959
1.11476E 01	4.23246E 02	2.98501E-01	6.24852E-02	3.27317E-02	2.16594E-03	1.25758	-0.54985	8.90345E-01	3.200E-02	1.3431
1.16596E 01	3.60214E 02	3.15253E-01	7.60689E-02	3.90455E-02	1.77953E-03	1.19166	-0.41347	8.27131E-01	1.600E-02	1.4450
1.21796E 01	2.89195E 02	3.46853E-01	9.82234E-02	4.79382E-02	1.31879E-03	1.12144	-0.26477	7.62313E-01	3.200E-02	1.6009
1.27555E 01	2.84449E 02	3.64570E-01	1.02443E-01	5.03771E-02	1.31428E-03	1.10690	-0.25584	6.51336E-01	1.280E-01	1.5963
1.32675E 01	2.84469E 02	3.78644E-01	1.04649E-01	5.20264E-02	1.33871E-03	1.09801	-0.24892	5.37769E-01	6.400E-02	1.5808
1.38435E 01	2.88265E 02	3.93001E-01	1.05517E-01	5.32714E-02	1.39131E-03	1.09219	-0.24879	3.94639E-01	1.280E-01	1.5542
1.43715E 01	2.73669E 02	4.13135E-01	1.13685E-01	5.69822E-02	1.30801E-03	1.07196	-0.19934	2.70817E-01	6.400E-02	1.5828
48835E 01	2.51832E 02	4.38484E-01	1.26391E-01	6.21547E-02	1.17011E-03	1.04605	-0.14080	1.55525E-01	1.280E-01	1.6385
1.50115E 01	2.46381E 02	4.45345E-01	1.29893E-01	6.35318E-02	1.13544E-03	1.03966	-0.11762	1.29893E-01	6.400E-02	1.6537

(a) Output from case with u_e specified.

Figure 10. Output from two-dimensional boundary-layer calculation.

UZ = 9.90272E 03
REZ = 3.02426E 05

AX	UTAU	DELTA	DELST	THETA	CF	UE/UZ	CP	DELST+R	DX	HTR
1.07500E 01	2.75498E 02	1.78631E-01	7.00000E-02	2.57929E-02	7.69997E-04	1.35316	-0.76251	9.52500E-01	1.000E-03	2.0173
1.12590E 01	1.72452E 02	2.21248E-01	9.82041E-02	3.13578E-02	3.41453E-04	1.28532	-0.60536	9.09175E-01	3.200E-02	2.4438
1.17710E 01	1.02738E 02	2.72118E-01	1.31509E-01	3.68020E-02	1.33273E-04	1.23465	-0.49654	8.65866E-01	6.400E-02	2.8961
1.22989E 01	1.05375E 01	3.66813E-01	1.97622E-01	4.25704E-02	1.51238E-06	1.19521	-0.40754	6.37636E-01	3.200E-02	3.8996
1.28109E 01	-6.15976E 01	4.95472E-01	2.82612E-01	4.58045E-02	-5.33745E-05	1.18032	-0.37411	8.20429E-01	6.400E-02	5.3088
1.33229E 01	-8.47186E 01	5.84193E-01	3.53071E-01	4.72912E-02	-1.11728E-04	1.17405	-0.36907	7.72345E-01	6.400E-02	6.5401
1.38489E 01	-1.11768E 02	6.55643E-01	4.22766E-01	4.98904E-02	-1.49161E-04	1.16670	-0.36175	6.98042E-01	1.280E-01	7.5262
1.44109E 01	-9.81451E 01	7.41305E-01	4.55544E-01	5.46883E-02	-1.42133E-04	1.15448	-0.35451	6.02825E-01	6.400E-02	7.4178
1.49229E 01	-8.10224E 01	7.38653E-01	4.43086E-01	6.09142E-02	-1.01259E-04	1.13233	-0.34828	4.62372E-01	6.400E-02	6.4475
1.54349E 01	-3.81512E 01	6.79185E-01	3.81732E-01	6.98739E-02	-2.38370E-05	1.10291	-0.23514	3.81732E-01	6.400E-02	4.7774
1.59469E 01	3.55697E 01	6.16782E-01	3.13125E-01	7.82838E-02	2.31262E-05	1.07668	-0.17348	3.13125E-01	6.400E-02	3.4571
1.64905E 01	8.86549E 01	5.84858E-01	2.68717E-01	8.26252E-02	1.39952E-04	1.06276	-0.13369	2.68717E-01	6.400E-02	2.7736
1.70025E 01	1.37914E 02	5.60358E-01	2.29902E-01	8.35395E-02	3.40719E-04	1.05992	-0.12697	2.29902E-01	3.200E-02	2.3093
1.75921E 01	1.73072E 02	5.55255E-01	2.07517E-01	8.37616E-02	5.36986E-04	1.05956	-0.12222	2.07517E-01	6.400E-02	2.0520
1.80100E 01	2.01755E 02	5.50656E-01	1.89600E-01	8.23511E-02	7.21649E-04	1.06483	-0.13313	1.89600E-01	1.280E-01	1.8930

(b) Output from case with δ^* specified.

Figure 10. Concluded.

```
BLAHA,CHAMBERLIN AND BOBER  6524  BOATTAIL-STING
INVISCID FLOW ONLY
TRANSONIC FLOW WITH WEAK SHOCK ON AFTERBODY
   -1    0    0
    1.4       0.9
   53
    0.0       0.0
    0.25      0.085
    0.50      0.17
    0.75      0.255
    1.0       0.34
    1.5       0.49
    2.0       0.64
    4.0       1.2
    6.0       1.68
    8.0       2.13
   10.0       2.56
   12.0       2.92
   14.0       3.24
   16.0       3.5
   18.0       3.65
   20.0       3.80
   22.0       3.91
   24.0       4.0
   26.0       4.0
   30.0       4.0
   35.0       4.0
   40.0       4.0
   45.0       4.0
   50.0       4.0
   50.4       4.0
   50.5       3.9997
   50.7       3.997
   51.0       3.988
   51.25      3.9759
   51.5       3.9597
   51.75      3.9392
   52.0       3.9146
   52.5       3.8525
   53.0       3.7733
   53.5       3.6767
   54.0       3.5624
   54.5       3.4298
```

(a) First 43 cards.

Figure 11. Input data for inviscid-flow calculation on body of figure 4.

```
55.0        3.2786
55.5        3.1080
56.0        2.9175
56.5        2.7061
57.0        2.4835
57.5        2.2609
58.08       2.0
58.5        2.0
59.0        2.0
59.5        2.0
60.0        2.0
60.5        2.0
61.0        2.0
62.0        2.0
63.0        2.0
64.0        2.0
51   31    10     0      0     0     0
 0.25       0.84      58.08      80.0      58.08
```

(b) Remaining 18 cards.

Figure 11. Concluded

NOMENCLATURE

A	factor defined by equation (13)
A_{ij}	coefficients in equations (38), (39) and (40) to (42)
a	speed of sound
B	factor defined by equation (14)
C	Chapman-Rubesin parameter, equations (22) and (27)
C_f	skin-friction coefficient
C_p	surface pressure coefficient
H	total enthalpy
H_{tr}	transformed boundary-layer shape factor, equation (44)
k	factor denoting two-dimensional ($k = 0$) or axisymmetric ($k = 1$) flow
L	reference length
M	Mach number
P	Prandtl number
p	pressure
r	radius
S	total enthalpy parameter, equation (4)
s	squared error factor, equation (49)
T	temperature
T_s	factor in Sutherlands viscosity relation, equation (28)
t	axisymmetric transformation factor, equation (15)
U,V	transformed velocity components, equations (18) and (19)
U_β	wake velocity factor, equation (32)

NOMENCLATURE (CONTINUED)

U_τ	friction velocity, equation (33)
u,v	velocity components of physical flow field, figure 1
$\tilde{u},\tilde{v}$	transformed velocity components, equations (9) and (10)
X,Y	transformed coordinates, equation (17)
x,y	coordinates of physical flow field, figure 1
x_p	axial location of peak pressure downstream of boattail
x_s	axial location of separation point
$\tilde{x},\tilde{y}$	transformed coordinates, equations (5) and (6)
Y^+	coordinate of logarithmic part of boundary layer, equation (34)
α	damping factor for viscid-inviscid iterations, equation (48)
β	eddy-viscosity factor, equations (35) to (37)
γ	ratio of specific heats
δ	boundary-layer thickness
δ^*	boundary-layer displacement thickness, $\int_0^\delta \left(1 - \frac{\rho u}{\rho_e u_e}\right) \frac{r}{r_w}\, dy$
δ_k^*	boundary-layer displacement thickness, $\int_0^\delta \left(1 - \frac{u}{u_e}\right) dy$
θ	angle of body surface with the axis; also boundary-layer momentum thickness
λ	constant in Sutherlands viscosity law, equation (28)
μ	molecular viscosity
ν	μ/ρ
ρ	density

NOMENCLATURE (CONCLUDED)

τ shear stress

ψ stream function

SUBSCRIPTS

e refers to boundary-layer edge

I refers to inviscid flow

i refers to incompressible flow

o refers to reference conditions

T refers to turbulent boundary layer

t refers to transitional boundary layer; also refers to stagnation conditions

V refers to viscous flow

w refers to the wall or solid boundary

x,y denotes differention with respect to x or y